Tracking of grid voltage envelope and flicker using phase locked loop and Kalman filter technique.

A thesis submitted to
Department of Electrical, Electronic & Communication Engineering
Military Institute of Science and Technology (MIST)
In partial fulfillment of requirement of the degree of
Bachelor of Science of Electrical, Electronics & Communication Engineering

By

Md. Naymur Rahman	**Student ID: 201416017**
Quazi Aquib Ferdaus	**Student ID: 201416045**
Mubashwir Rafsan	**Student ID: 201416046**

Under the Supervision of:

Dr. Md. Shamim Reza
Associate Professor
Department of Electrical and Electronic Engineering
Bangladesh University of Engineering and Technology

Department of Electrical, Electronic and Communication Engineering

Military Institute of Science and Technology (MIST)

December, 2017

CERTIFICATION OF APPROVAL

The thesis entitled “Tracking of grid voltage envelope and flicker using phase locked loop and Kalman filter technique.” submitted by Md. Naymur Rahman (201416017), Quazi Aquib Ferdaus (201416045) and Mubashwir Rafsan (201416046) , has been accepted as satisfactory in partial fulfillment of the requirements for the degree of BACHELOR OF SCIENCE IN ELECTRICAL,ELECTRONIC & COMMUNICATION ENGINEERING.

____

Dr. Md. Shamim Reza
Associate Professor
Department of Electrical & Electronic Engineering
Bangladesh University of Engineering & Technology.

DECLARATION

We thereby declare that thesis work is our work. Wherever contribution of others are involved, every effort has been made to indicate this clearly, with due reference to the literature, and acknowledgement of collaborative research and discussion. This paper is made for academic purpose and has not been submitted before any other objective.

Authors:

Md. Naymur Rahman
Student ID: 201416017
EECE-12
MIST

Quazi Aquib Ferdaus
Student ID: 201416045
EECE-12
MIST

Mubashwir Rafsan
Student ID: 201416046
EECE-12
MIST

Acknowledgement

All praise goes to the Almighty for giving us the drive to finish this thesis work in due time.

We would like to thank our thesis supervisor Dr. Md. Shamim Reza, Associate Professor, Department of Electrical and Electronic Engineering (EEE), Bangladesh University of Engineering and Technology (BUET), for giving us his precious time and generously helping us with his suggestions, ideas and providing well defined guidance throughout the thesis work. We are grateful to him for understanding us and giving us freedom to do things our way. In a way he pushed us so that we could reach our full potential and really exploit out capabilities and this also made our work more enjoyable and fruitful.

We would also like to thank our teachers of MIST for believing in us and giving us a chance to work with our thesis supervisor. They were very patient and understanding about our situations.

We would also like to thank our families. Without their love and support we couldn't have finished the thesis work. They were a great source of encouragement in our work.

Finally, we are grateful to our friends and well-wishers who believed in us and gave us encouragement all throughout the thesis work.

Abstract

Accurate estimation of instantaneous flicker level (IFL) of the grid voltage is crucial for design and implementation of electrical devices. The grid voltage amplitude, frequency, and phase fluctuate from its nominal value due to flicker which can be estimated from its envelope. In the proposed technique, the enhanced phase locked loop (EPLL) is integrated with the Extended Kalman filter (EKF) to estimate flicker. An EPLL based algorithm is developed for extracting the grid voltage envelop and an EKF based algorithm is adopted for estimation of IFL.

In this thesis, a combination of EPLL with EKF is used to directly extract the IFL from the grid voltage. The developed EPLL-EKF technique has been tested in MATLAB environment for different types of imbalances and distortions. This system works perfectly even when the fundamental frequency or the flicker frequency is varying with time. This method is capable of handling non-linear variations of flicker where as other existing methods require modification.

Table of Contents

List of Figures

List of Abbreviations

Abbreviation	**Description**
AC	Alternating Current
CMC	Cascade-multilevel converter
DG	Distributed Generation
DFT	Discrete Fourier Transform
EKF	Extended Kalman Filter
EPLL	Enhanced PLL
FLL	Frequency locked loop
FC-TCR	Fixed Capacitor Thyristor Controlled Reactor
IFL	Instantaneous flicker level
KF	Kalman Filter
LKF	Linear Kalman Filter
PQ	Power quality
PQC	Power Quality Conditioner
PLL	Phase-Locked Loop
$\mathbf{P_{ST}}$	Short-term flicker severity
$\mathbf{P_{LT}}$	Long-term flicker severity
RSW	Resistance spot welding
RMS	Root mean square

STATCOM	Static synchronous compensator
TCR	Thyristor Controlled Reactor
UPQC	Unified Power Quality Conditioner
VCO	Voltage-Controlled Oscillator
VAR	Volt-ampere Reactive

List of Symbols

Φ: Luminous flux

X: Exponent value depending on light source type

$\emptyset_0$: Phase angle of the input signal

ω_0: Frequency of oscillation

$\dot{\omega}$: Rate of change of frequency

U_0: Peak amplitude of the input signal

$\dot{U}_0$: Rate of change of amplitude

s: Unity sinusoidal signal

$s^{\perp}$: Normalized quadrature (90◦ phase-delayed) signal

u: The input signal of EPLL

y: Fundamental component and filtered version of u

$y^{\perp}$: Quadrature of fundamental component

φ : The phase angle of fundamental component

e: Distortions and noise

μ: Gain value of EPLL

ω_n: The nominal value of input frequency

ζ : Damping ratio

ω_r: The bandwidth corresponding to the phase/frequency

Ts : Sampling time

K: The sampling instant

f : Fundamental frequency of grid voltage

AF: Flicker amplitude

fF: Flicker frequency

θ : Initial phase angle of the voltage flicker

P : Damping constant

A_0: Amplitude of the fundamental frequency

w_1: Initial angular frequency of voltage signal

ω_{ft}: Angular frequency associated with the flicker component

ϕ: Phase angle of the system

ϕ_f: Phase angle of the fundamental voltage

x1F: State corresponding to IFL in grid voltage

x2F: State corresponding to quadrature component of IFL

x3F: State corresponding to flicker frequency

x4F: State corresponding to amplitude of fundamental voltage waveform

DF: State transition matrix

HF: Measurement matrix

P: Error covariance matrix

Q: Process noise covariance matrix

K: Kalman Filter gain

R: Measurement noise

I: Identity matrix

e_k^-, e_k: Error in previous and post states of EKF

$\tilde{e}_{x_k}$: Approximate measurement error

$\tilde{e}_{z_k}$: Approximate residual

P_k^-, P_k: Error covariance's in previous and post states

$\hat{x}_k^-, x_k$: Previous and Post state estimates

$\tilde{x}_k$: Approximate state

z_k: Measurement at state K

$\tilde{z}_k$: Approximate measurement

w_k: Process noise

v_k: Measurement noise

Chapter 1: Introduction

This chapter introduces the flicker and its brief description in section 1.1. It is followed by types of flicker and a brief example of how disturbance in electric systems are caused by flicker is given in section 1.2 and 1.3 respectively. How it occurs and the sources of flicker occurrences in the system is shown in section 1.4. In section 1.5 the main objective of flicker estimation is brought forward including what techniques we had adopted. The thesis methodology and techniques for the thesis are described in section 1.6. Finally how the thesis has been organized is shown in section 1.7.

1.1 Flicker familiarization

Flicker is the change in visible light due to the rapid change and fluctuations of the power supply, it is basically a voltage drop across the source impedance of the grid by changing the load current of an electrical machine, facilities or factories that will result in voltage drops [1-13]. The visible change in brightness or power consumption of lamp or the electric component due to rapid fluctuations in the voltage of power supply is known as voltage flicker [2-4, 14-17]. These can be harmful for sensitive electronic equipment and industrial processes that rely on constant electrical power [18]. Flicker can occur for different duration of intervals such as 2 min minimum to 10 min maximum or more [19-21]. Unlike other electrical problems flicker can be seen by the naked eye, it is easy to recognize because it causes the light in common households to change their brightness quite rapidly.

There are many sources of voltage flicker in a specific system produced by severe load changes due to arc furnaces, arc welders, to milder ones such as: starting industrial motors, pumps, elevators, and fans [5, 22-24]. Such severe changes of the loads connected cause a small voltage variation which is recurring of about ±5% to ±10% in amplitude and 1–50% in frequency of the system voltage envelope [25].

A figure showing voltage fluctuation for an interval of 0-200ms is given below.

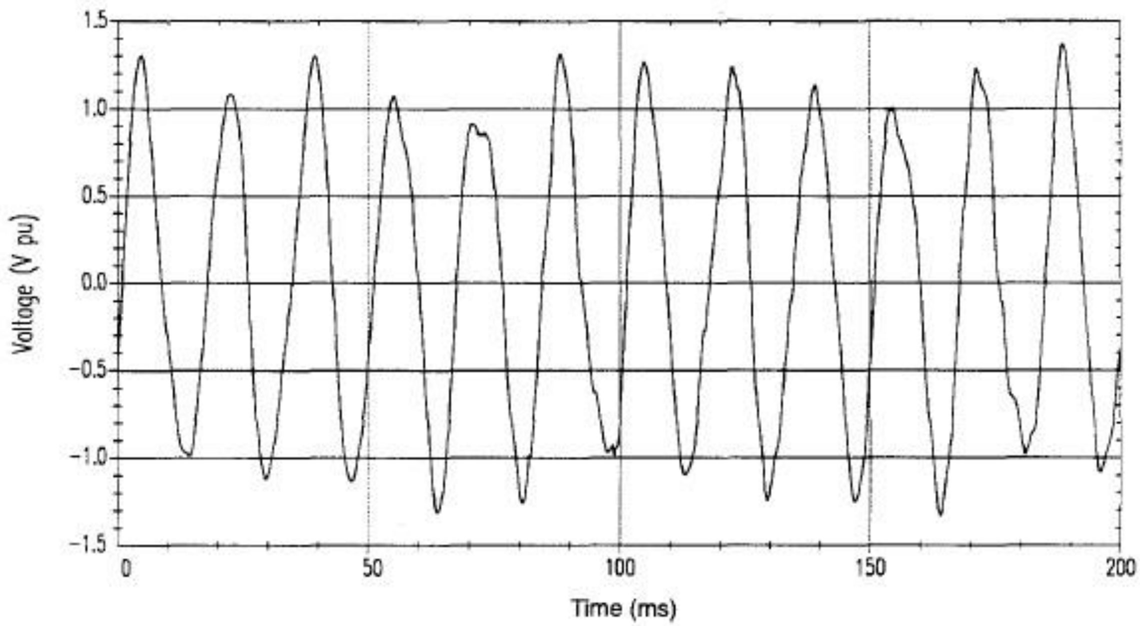

Figure 1.1: Voltage fluctuation in grid voltage for an interval of 0-200ms [26].

Flicker is a subjective phenomenon in day to day life. Consequently, it's difficult to estimate the direct cost of its effect. Nevertheless, the phenomenon affects the ability to provide power supply that is steady and consistent to the consumers. Certainly, it can affect productivity in an office or factory, but the damages done by flicker usually depends on the cost of mitigating it when the complaints are introduced [27].

Developments in power electronics, in particular in semiconductor device manufacturing, has enabled the practical realization of voltage dynamic stabilization systems of larger rated power, while at the same time minimizing investment and operational costs [28, 29]. The availability of equipment with the ability to execute complex control algorithms also allows the use of diverse functions, including dynamic voltage stabilization [30,31].

1.2 Types of Flicker

The voltage flicker involves the system RMS voltage variations, and the frequency at which the variations occur. There are two general categories of flicker phenomenon [18, 32-34]. They are-

1.2.1 Cyclic flicker

In a power system consisting of high voltage loads such as spot welders, compressors, or arc welders cause occurrence of cyclic flicker due to periodic voltage fluctuations of the loads. Cyclic flicker are repetitive. The cyclic voltage flicker magnitude component varies randomly [35, 36]. Cyclic voltage flicker occurs because of slow change in the voltage magnitude in the frequencies between 0.5 Hz to 25 Hz, the phenomenon can be seen on the fundamental signal envelope.

1.2.2 Non-cyclic flicker

The occasional voltage fluctuations of some time-varying loads, such as starting of large motors, arc furnaces, welders, and ac choppers cause Non-cyclic flicker [35, 36]. Non-cyclic flicker may also occasionally occur with cyclic flicker in some cases in arc furnaces, welders, and ac choppers.

Both cyclic and non-cyclic flicker appear in electric systems and their occurrence are uncertain due to the amount of power consumption are not always the same by the above mentioned high voltage loads [32, 37].

Examples of cyclic flicker and non-cyclic flicker are shown in Figures-

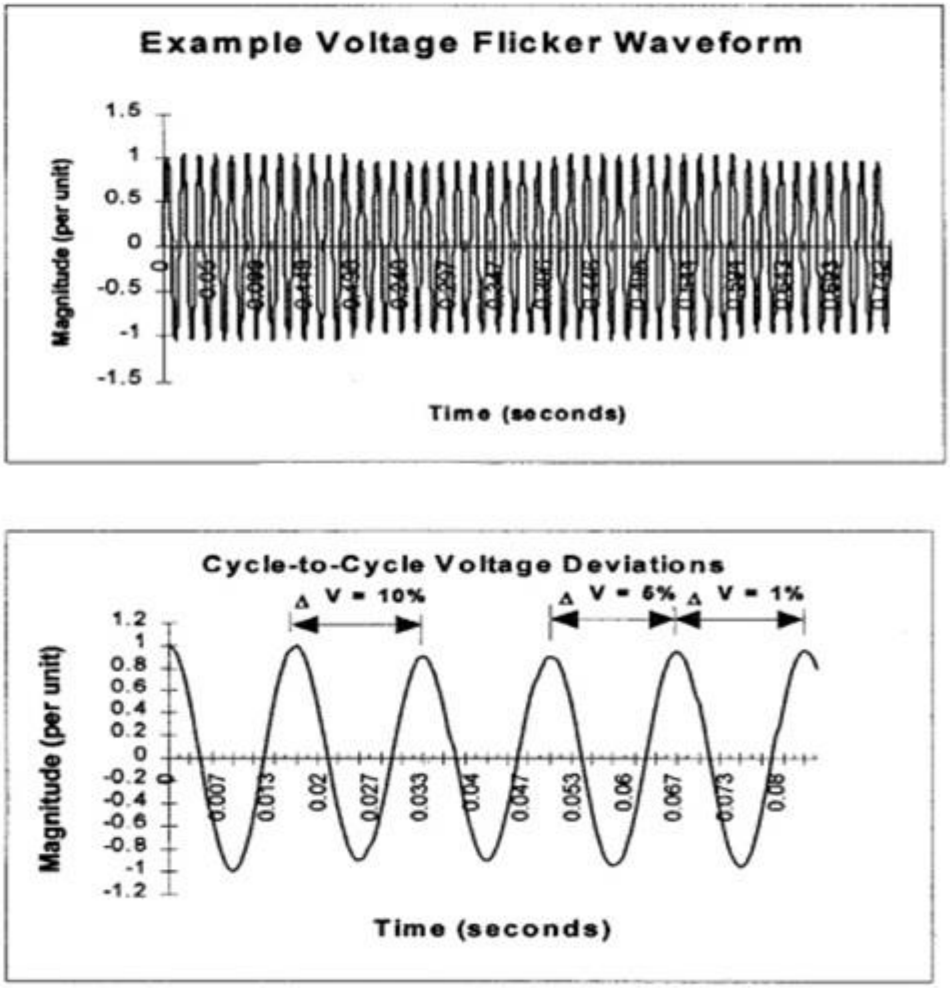

Figure 1.2.1: Cyclic and Non-Cyclic Voltage Flicker[38].

Any flicker measurement system must be able to accurately characterize the levels of cyclic and non-cyclic flicker [39].

Instantaneous flicker levels are characterized by two parameters that determine voltage fluctuations are the short-term flicker severity (P_{ST}) and long-term flicker severity (P_{LT}) index [40]. These factors refer to voltage fluctuation effects on lighting and their influence on humans. A short brief of both are given below:

1.2.3 Short-term flicker severity(P_{ST})

The short-term flicker is the measure over a short period of a few minutes of how damaging and irritating flicker is thought to be. Problems may be caused by events of consistent minor flicker or occasional major flicker. The statistical treatment used to obtain P_{ST} is intended to model the way humans react. A value measured over 10 minutes that characterizes the likelihood that the voltage fluctuations would result in perceptible light flicker [41]. A value of 1.0 is designed to represent the level that 50% of people would perceive flicker in a 60W incandescent bulb [42]. A graphical representation of short-term flicker is given-

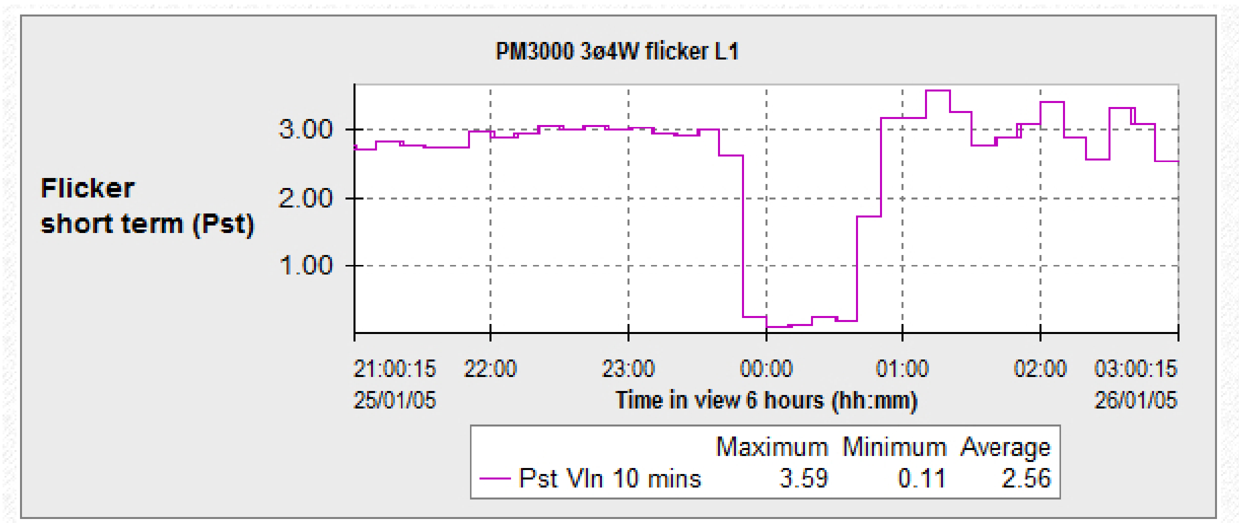

Figure 1.2.2: Graphical representation of P_{ST} [40].

1.2.4 Long-term flicker severity(P_{LT})

Long-term flicker severity is a further measure for cumulative irritation which is caused by very occasional gross flicker events of short terms, which may be too infrequent to cause meaningful P_{ST} results in such cases [41]. In the following graph, the measurement plotted every 10 minutes is the average flicker value of the last 2 hours a value derived from 2 hours of P_{ST} values [40]. A graphical representation of long-term flicker is given-

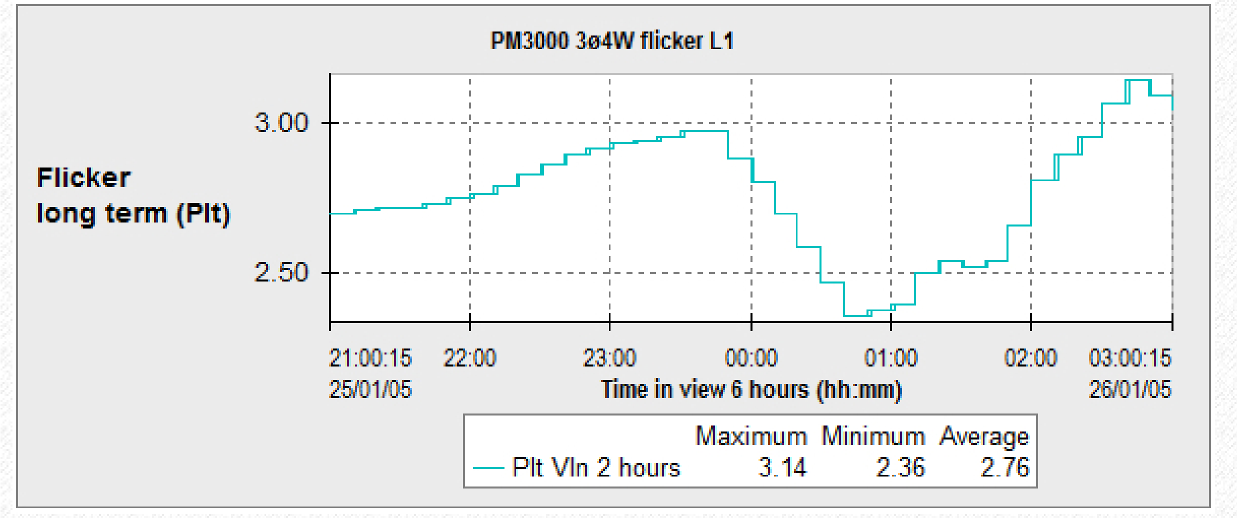

Figure 1.2.3: Graphical representation of P_{LT} [40].

IEC 61000-2-2 specifies the following flicker compatibility levels [41]:

1 Compatibility level for short-term flicker (P_{ST}) is 1.0.

2 Compatibility level for long-term flicker (P_{LT}) is 0.8.

In general there are essentially four different types of flicker in case of light illumination which may indicate irregular, load induced disturbances on the 230V power line:

1.2.5 Load induced flicker

These types of Incidental variations of the light intensity cannot be directly related to regular events happening in the electric power grid. They are mainly produced by large wind turbines [43]. The duration of the flicker and interval are varying from tens of milliseconds to seconds or minutes in the system.

1.2.6 Dimmer incompatibility flicker

These types of flickering event comprise of continuous flickering at intervals of 2 to 10 variations per second, in combination with a dimmer circuit [44].

1.2.5 CAB induced flicker

These types of flicker events are which happen regularly, several times per day at well-defined times. It happens in combination with dimmer circuits. The duration of the flicker and interval are varying in the order of a few seconds. CAB induced flicker is visible through naked eye but due to change in frequency level they might not be visible for certain variations of high frequency.

1.2.6 Stroboscopic flicker

Flicker variations consisting of continuous flickering at intervals of 100 or 120 variations per second are mainly known as stroboscopic flicker. This type of flicker is not visible for human eye because of higher frequencies. Stroboscopic flicker may no longer be directly visible but can be detected with fast eye or head movements or by moving objects quickly [45].

1.3 Disturbances due to flicker

Flicker is one of the most significant effect of voltage fluctuation as it can affect the production environment. Voltage fluctuations may cause considerable financial cost by disrupting production process and it also effects electrical and electronic equipment.
The effects of flicker on susceptible equipment are discussed below.

1.3.1 Light sources

Light sources are sensitive to voltage supply changes or flicker as the luminous flux is directly proportional to the applied voltage. The equation of luminous flux is given below:

$$\Phi = V^X$$

Where:
Φ = luminous flux
V = applied voltage
X = exponent value depending on light source type

For example, the value of X is basically between 3.1-3.7. Meanwhile, X is lower about 1.8 for fluorescent and discharge lamps because incandescent lamps are more sensitive to voltage fluctuations than discharge lighting equipment and fluorescent lamps [46].

Voltage fluctuations cause variations of the light output from incandescent and fluorescent lamps. Which shows a visual impression of unsteadiness of a light's flux, whose luminance fluctuates with time.

A regular or irregular voltage change of 0.5%-1.0% consisting a frequency of about 6 to 8 Hz can result to flicker which can be observed in the light output of an incandescent lamp [47]. So, flicker affects the reaction of the brain and by causing discomfort to the eyes. Worst case, it can even result to accidents as it affects the ergonomics of the production environment by causing personnel fatigue and reduced concentration levels.

1.3.2 Electric machines

i. Synchronous Motors and Generators

Voltage fluctuations at the terminals of Synchronous Motors and Generators lead to the following:

1. Increase in losses
2. Premature wear of rotors
3. Changes in torque and power
4. Hunting

ii. Induction Motors

In case of induction motors, voltage fluctuations at the terminals may cause changes in torque and there is also a slight change in slip, thus production process is affected. In the worst case, fluctuations could result to excessive vibration. Thus the mechanical strength of the motor is reduced and the motor service life is shortened [48]. In industries induction motors thus have lower service life due to flicker.

1.3.3 Electro-heat Equipment

Voltage fluctuations will cause lower operational efficiency to all heating equipment that require stable voltage supply. Their efficiency drops according to the amount of voltage fluctuation [49]. For example, an electric arc furnace would require a longer melt time if the voltage supply is not stable [13, 35].

1.3.4 Electrolyzers

Flicker present in electrical supply can reduce both the useful life and the operational efficiency of the electrolyzer equipment. The flicker or voltage fluctuations thereby increase maintenance and in addition, elements of the high-current supply line can become significantly degraded [50]. The repair cost is also increased.

1.3.5 Static Rectifiers

The effect of voltage fluctuations in static rectifiers decrease the power factor and generate variations in non-characteristic harmonics and inter-harmonics. Because of flicker it can result in commutation failure and damage to system components in the case of drive braking in case of an inverter mode [49].

1.3.6 Other Devices

Furthermore, other effects of voltage fluctuations include [46]:

1. Malfunction in security system;
2. Unwanted triggering of UPS systems;
3. Computerized or automatic machines may involve in producing defective parts;
4. Testing equipment may give inaccurate data;
5. Relays and contactors may not operate in exact time;
6. Motor speed may not be consistent;

1.4 Flicker Occurrence & causes

Power interruptions lasting less than one minute are mainly known as flickers, and they may occur at any time. They can be caused by a number of factors, including-

- **Lightning strikes:** If lightning strikes overhead high voltage lines, the sudden increase in voltage will cause arcing to earth across the insulator and as the arc has a very low resistance the line will be basically shorted to ground as a result flicker will occur across the high voltage line.
- **Damaged electrical equipment:** If electrical equipment's or a part of it damaged it might take more power from the line then necessary which causes flicker but this is not that much of a concern as protective devices are there in case of such a problem.
- **Arc welders:** Arc welders are similar to electric furnaces it just has a smaller scale. When it is turned on it continuously draws power and can cause flicker.
- **Electric arc furnace:** Electrical arc furnaces are a main source of flicker. The flicker associated with electric arc furnaces are a mixture of cyclic and non-cyclic flicker.
- **Spot welders:** Resistance spot welding (RSW) is a process in which contacting metal surface points are joined by the heat obtained from resistance to electric current. It is a subset of electric resistance wielding.
- **Static frequency converters:** A frequency changer or static frequency converter is an electronic or electromechanical device that converts alternating current of one frequency to alternating current of another frequency. The device may also change the voltage, but if it does, that is incidental to its principal purpose.
- **Rolling mill drives:** Rolling mill drives are used to reduce the thickness of a metal sheet is related to metal-works. As the rollers require a large power to work the cause flicker but precautions are taken so that flicker does not occur.
- **Large motor (Starting):** During the starting of a large motor it draws a huge current from the power line which momentarily causes flicker.

- **Compressors:** Compressors are electromechanical devices which are a vital part of many industries. But as the compressor turns on it draws a large amount of power from the power line.
- **Cycloconverter:** A cycloconverter or a cycloinverter converts a constant voltage, constant frequency AC waveform to another AC waveform of a lower frequency by synthesizing the output waveform from segments of the AC supply without an intermediate DC link. During the working process it produces flicker which is incidental to the working principal.

Similar to a circuit breaker in homes, a flicker occurs when our system automatically shuts off electricity to isolate the problem area. When the line is cleared the system resets itself and electrical service is quickly restored. Briefly shutting off power and isolating the problem helps prevent damage to the electric system during the occurrence of flicker in the system, so if not it could result in a larger outage and effect many more customers.

1.5 Objective of the thesis

In a high voltage system Flicker is the fluctuation or sudden change of the magnitude of the grid voltage. This sudden fluctuation or jumps include deterministic and random variations. The size and type of the load determine the occurrence of the instantaneous voltage flicker and the flicker level. Arc furnace operation is one of the most recognized source of voltage flicker. The main objective of the thesis is to track the fundamental voltage flicker amplitude generated in the power system. We had adopted the EKF technique for estimation of the instantaneous voltage flicker magnitude, frequency and phase. In this paper, we have demonstrated an adaptive strategy to address the probability of flicker. The EPLL tracks the time-varying grid voltage fundamental frequency adaptively. The fundamental voltage envelope is obtained from the grid voltage waveforms as provided by the EPLL and is fed to the extended Kalman filter (EKF) to extract the instantaneous flicker level (IFL). As Arc furnaces and other High voltage system such starting of large motors, welders, ac choppers, spot welders, and compressors are sources of consuming much greater extent of the generation voltage the occurrence of flicker is much higher and can be traced using this technique. This thesis paper demonstrates a method of measuring the low frequency distortion of the 50 Hz signal using a Kalman Filtering approach. The outputs of this method are the voltage flicker amplitude, frequency and phase angle. This is how the change in different parameters in the input signal and EKF states helps extract the voltage flicker to an acceptable limit. Details of the model and the results of the approach for typical cases are presented. Variations of the frequencies in the grid voltage are extracted and in case of different types of flicker such as sinusoidal, sawtooth, triangular and square variation of flicker can also be extracted in the EKF method.

1.6 Thesis Methodology

The thesis comprises of step by step estimation of the instantaneous grid voltage flicker. At first a grid voltage had been generated in the MATLAB as input of the EPLL. Using EPLL we had extracted the envelope of the grid voltage. The instantaneous grid voltage equation had been set up such that it contained the disturbance or flicker which is to be extracted. We have taken the nominal value of the grid voltage frequency. The EPLL gains have been set up accordingly and the error signal is updated corresponding to the update of the input signal. The envelope extracted is the EKF input signal for the estimation of instantaneous flicker present in the grid voltage. The time update stage and measurement update stage in the EKF technique is updated for different sampling instances. The gain of the EKF and the states had been updated in different sampling instances and by comparing the values of k^{th} and $(k+1)^{th}$ sampling instant the state indicating IFL present is estimated including the amplitude and frequency of the flicker. The thesis also comprises flicker estimation for different variations of flicker waveforms such as sinusoidal, sawtooth, triangular and square.

1.7 Thesis Organization

The thesis titled "Tracking of grid voltage envelope and flicker using phase locked loop and Kalman filter technique" has been organized as follows-

Chapter 1: The chapter is entitled as introduction and it gives in brief familiarization with the grid voltage flicker and the occurrence and causes of flicker in the grid voltage. The problems in electrical components and systems due to flicker is also described in this chapter. The objective of the thesis and the thesis methodology are also briefed in the following sections.

Chapter 2: In this chapter different existing techniques are described. Different types of flicker and their mitigation techniques are also discussed in this section.

Chapter 3: A brief description of Kalman filter and how it helps to predict the next value from the existing data are given in this chapter. Basic algorithm of Kalman filter is also shown in this section and followed by familiarization with Discrete and Extended Kalman filter. EPLL and its basic equations are also described in this section. In this chapter there are two sections describing how the process of estimating IFL in the grid voltage had been carried out. The first section shows how we had extracted the envelope of the grid voltage and the second section shows how we had estimated the IFL present using EKF technique.

Chapter 4: In chapter four the simulation results for the proposed EPLL-EKF technique of flicker estimation has been presented. These simulations involve numerous variation of flicker waveforms, frequency variation of nominal fundamental grid voltage frequency and flicker frequency.

Chapter 5: The chapter represents the conclusion summarizing the thesis work and suggestions of future aspects.

Chapter 2: Literature Review

In this chapter different existing techniques for flicker estimation has been described in section 2.1. Section 2.2 shows different types of flicker mitigation techniques.

2.1 Existing techniques

With numerous applications of grid-connected systems increasing day by day, the importance of flicker estimation and mitigation has become a crucial aspect. A large number of researches has been developed in this field which has produced various methods of flicker estimation.

In order to estimate the flicker in grid voltage a system is required to extract the envelope, it is then applied as input to another tracking system to estimate the future value of IFL from the existing data. A few methods of flicker estimation are as follows:

2.1.1 Flicker waveform model

The modeling of a voltage flicker is important before implementing any envelope tracking method. The disturbance in a distribution line can be figured out by getting information of the amplitude, the angular frequency and the phase angle of the disturbance. The amplitude may vary with respect to the source of production. Amplitude can be in the form of step, square, ramp or even sinusoidal by putting the values of the unknowns in the voltage envelope of the disturbance in the grid. The equations used in this method are as follows [52-54]-

$$v(t) = A(t)\sin(w_1 t + \phi)$$

This equation is used to get the value of voltage and its envelope. Here, $A(t)$ is the amplitude of the voltage w_1 is the initial angular frequency and ϕ is the phase angle of the system. The equation above gives us the envelope but if the disturbance is a sinusoidal waveform then the equation changes to-

$$A(t) = A_0 + A_f(t)\sin(\omega_{ft} + \phi_f)$$

In this equation A_0 is the amplitude of the fundamental frequency. A_f is the frequency component of the flicker, ω_{ft} is the angular frequency associated with the flicker component and ϕ_f in the phase angle of the fundamental voltage.

Considering the differences of equations because of the inputs to track the envelope a form of equation has been developed it is-

$$v(t) = A(t)\{sinw_1 t\ cos\phi_1 + cosw_1 t\ sin\phi_1\}$$

$$v_{en} = A(t) = \sqrt{w_1^2 + w_2^2}$$

The voltage waveform is calculated by the $v(t)$ and finally the voltage envelope is made by v_{en}. w_1,w_2 are equal to $A(t)cos\phi_1$ and $A(t)sin\phi_1$ respectively. This model is capable of detecting most of the problems associated with power quality.

2.1.2 Frequency adaptive least square Kalman technique

This method uses a two- level mathematical model for getting the voltage waveform. The least squares part of this method is used to figure out the fundamental frequency of the voltage waveform and updates the estimated frequency of the voltage waveform. The Kalman filter along with the least square algorithm is used to predict the instantaneous voltage flicker level (IFL). The equation used to describe the voltage flicker is taken from the amplitude modulation the fundamental components of frequency. It can be written in the following manner [55]-

$$v_{AM}[kT_s] = (U_c[k] + m[k])\sin(w_0 kT_s + \theta)$$

Low frequency voltage fluctuation that originate from sources of flicker are represented by $m[k]$, they are called instantaneous flicker level (IFL). The portion of the equation associated with the voltage envelope is$(U_c[k] + m[k])$. If we want to calculate just the fundamental components of the system then we simply leave out $m[k]$ from the overall equation [56]. This procedure usually has two steps a voltage envelope tracking algorithm and an instantaneous frequency level prediction system. This system can also be put in a digital system. The system described here is basically a non-linear and non-recursive form of the system that we developed in this thesis work. Probably the best example of this method is a non- linear Kalman filter [57-60].

The least square algorithm is used to calculate the fundamental frequency of the voltage waveform and the Kalman filter along with the least square algorithm is used to update the system constantly with more updated and accurate values. This is the way this method predicts instantaneous flicker level (IFL).

2.1.3 Recursive least square method

The recursive least square method assigns different weights to different measurements. Usually the current measurement is weighted the heaviest. This is done so that the previous inputs put less and less effect on the output. The method is an extension of the non- recursive least squared method Kalman filter is a good example of this method. A recursive least error squares algorithm for power system relaying and measurement applications [53].

The recursive least square method is an algorithm that has been derived from the conventional non-iterative least squared method [52, 53]. This system basically employs a weighting scale λ that is updated every time a new output is received. Usually the most recent result is weighted the most so that the previous outputs can't have much effect on the present output. This system can be explained by two equations which are as follow [56, 61-64]-

$$\hat{\theta}(k) = \hat{\theta}(k-1) + P(k)\phi(k)[y(k) - \phi(k)^T\hat{\theta}(k-1)]$$

$$P(k) = \frac{1}{\lambda}[P(k-1) - \frac{P(k-1)\phi(k)\phi(k)^T P(k-1)}{\lambda + \phi(k)\phi(k)^T P(k-1)}]$$

Here,$\hat{\theta}(k)$, $\phi(k)$ and $P(k)$ are matrices of sizes $n \times 1$ for the first two components and $n \times n$ respectively. The above mentioned components are parameter estimation vector, connection vector and weighting matrix sequentially. $y(k)$, λ, n, k are measured signal, forgetting factor, number of variables and the order of sampled time respectively. The forgetting factor is utilized so that convergences can be faster. As the λ increases the previous results are slowly forgotten slowly and vise-versa. This method is an improvement to the previous method [53].

2.1.4 Flicker estimation using flicker meter

In this method a flicker meter is used to predict flicker. The flicker meter is composed of a composition of five functional blocks. The five blocks have their specific work and rely on the previous block for input. The five blocks are [65]-

1. **Input adaptor voltage:** This block has the function of taking the input voltage and adapting it to an internal reference voltage without changing the voltage fluctuation that are present in the original input signal.
2. **Squaring multiplier:** The purpose of this block is to recover the voltage fluctuations from the scaled input voltage by squaring the output from the previous block.
3. **Filters:** This block consists of a high-pass, low-pass and weighting filter. At first the DC components are subtracted from the previous blocks output. Then the signal is passed through a sixth order low-pass Butterworth filter after that it is passed through a first order high-pass Butterworth filter.
4. **Squaring and smoothing:** This block has a non-linear function. It first squares the signal then it is passed through a low-pass filter that has a resistor, a capacitor and a time constant. The output of this signal corresponds to Instantaneous flicker P_{ins}.
5. **Online statistical analysis:** In this block the statistical analysis is carried out for calculating P_{ins}. To figure out the severity of the flicker we need to know exactly how much time every magnitude of P_{ins} persists for.

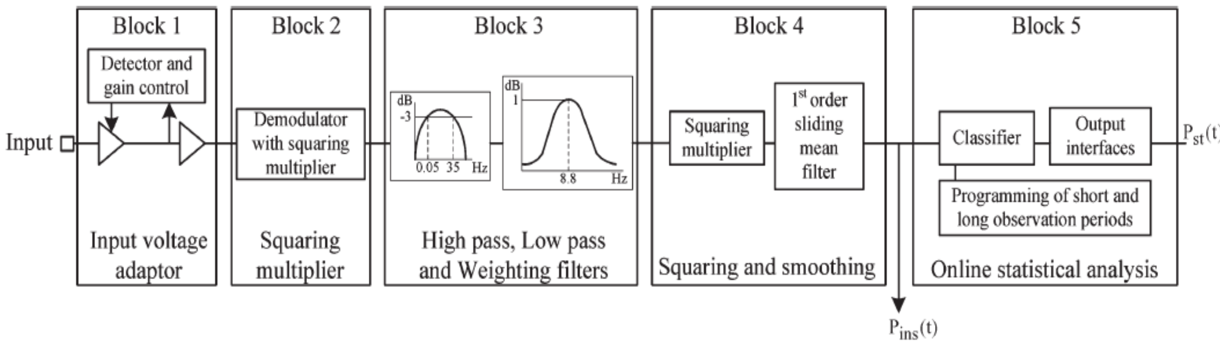

Figure 2.1: Block Diagram of a Flicker meter [66].

2.1.5 Flicker parameter calculation using voltage inter-harmonics

This method uses discrete Fourier transform (DFT) to get the parameters associated with voltage flicker and also estimates inter-harmonics at the same time. Using the odd points interpolation correction method it obtains the amplitude, frequency and phase angle of each frequency components. The procedure of this method is divided in a few steps [65-69]-

1. Using three points interpolation correction method the fundamental frequency f_0, amplitude m_0 and phase angle ϕ_0 is taken from the input signal $u(t)$.
2. Taking the time domain of the first step the fundamental signal is reconstructed using-

$$u_0(t) = m_0 \cos(2\pi f_0 t + \phi_0)$$

3. The $u_0(t)$ from the previous step is reduced of its fundamental components and the equation becomes-

$$u_1(t) = u(t) - u_0(t)$$

4. Then the three points interpolation correction method is used again to determine first inter-harmonics components f_k, m_k, ϕ_k of the signal from last step which was $u_1(t)$.
5. Using the information from the previous step the reconstruction of the signal is done in time domain using-

$$u_k(t) = \cos(2\pi f_k t + \phi_k)$$

6. After that the result from step three is subtracted from the result of step five. The equation then stands-

$$u_2(t) = u_k(t) - u_1(t)$$

7. Now the criterions are checked for convergence. If yes then the algorithm will stop there otherwise it will update the current signal and return to step four with the next inter-harmonics.
8. At last determining the frequency f_i , amplitude m_i , and phase angle ϕ_i of the input signal. Extracting the inter-harmonic pairs by the double-band property and the inter-harmonics-flicker frequency range. The parameters of flicker signal are calculated by the transform equations.

2.2 Flicker mitigation techniques

Several techniques have been developed to track and voltage flicker. For mitigation of voltage flicker there are several techniques to be applied and different systems to provide mitigation of the voltage flicker. Various kinds of mitigation techniques are demonstrated below-

2.2.1 Energy storage/smoothing

Obviously some sort of energy storage solution could be adopted or installed either at the point of connection to smooth the power fluctuations and hence reduce flicker if necessary [50]. There are many options and methods available for energy storage. Flywheels, hydraulic accumulators and other mechanical storage solutions are available today [51, 70-72]. Electrical storage solutions can be taken into account such as capacitors, battery energy storage etc. [72]. The storage system must be fast acting and rated for the amplitude of the power fluctuation during faults. It will also be subjected to multiple cycles during its lifetime. This solution may have additional costs and produce some losses in the overall system with also a much higher initial cost of installation which may be unacceptable [50].

2.2.2 FC-TCR (Fixed Capacitor Thyristor Controlled Reactor)

Static VAR compensators having fixed capacitor and thyristor controlled reactor are called FC-TCR. They are used to improve the overall stability of the system. In power system it used to stabilize the effects of flicker. It is a non-linear system. The capacitor is fixed that’s why it will produce a fixed amount of reactive power and the thyristor controlled reactor will consume that reactive power. It works by changing the firing angles of the TCR to produce variations of reactive power in the system. This solution is an example of indirect compensation technique. With the help of the required function of voltage stabilizer or reactive power compensator, the value of the sum of two current components is controlled. For example, to control the fundamental harmonic of the capacitor current, the capacitor is operated as a filter or as switched capacitor steps. For controlling the fundamental harmonic of the reactor current the use of a thyristor AC switch comes in hand [73].

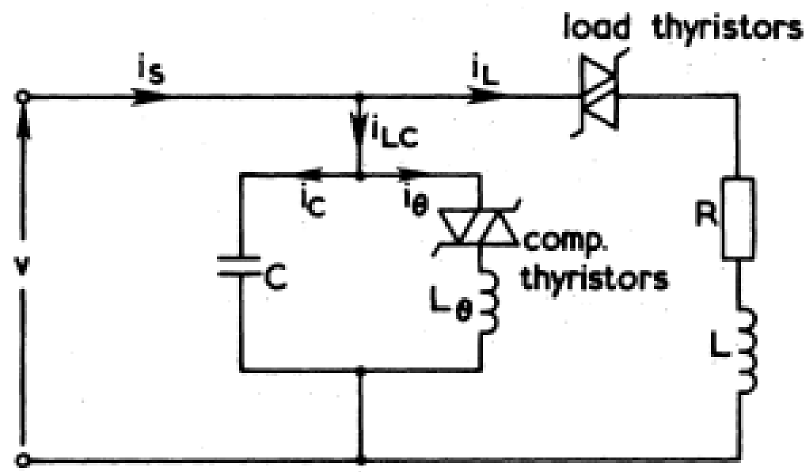

Figure 2.2: Diagram of a FC-TCR [73].

2.2.3 Cascade-multilevel converter (CMC) based Static synchronous compensator (STATCOM)

It is a fast compensating or neutralizing technique that includes reactive power source that's applied on the transmission or distribution system to reduce voltage variations such as flicker [75-77]. It is basically a structure containing multilevel converters cascaded together along with STATCOM's and are altogether connected to a winding of a transformer to reduce the voltage instabilities of a system.

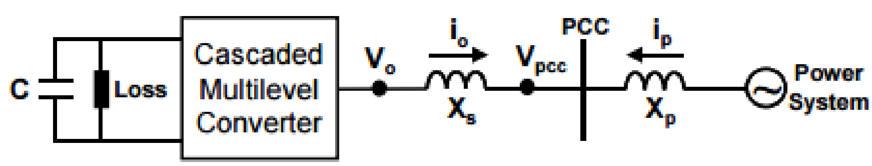

Figure 2.3: Single line diagram of a CMC based STATCOM [78].

2.2.4 Distributed Generation (DG)

The DG system refers to power generation at the point of consumption and generating power on-site, rather than centrally [79, 80]. It eliminates the cost, complexity, interdependencies and in efficiencies associated with transmission and distribution of a power system [81-83].

2.2.5 Unified Power Quality Conditioner (UPQC)

It is a combined system of shunt and active-series filters. A power quality conditioner is a device intended to improve the quality of power that is delivered to electrical load equipment [84]. There are three types of power quality conditioner's –

2.2.5.1 Shunt active power filters

This class of filter configuration is widely used in industrial processes [85-91]. It is connected to the main power circuit, and it is shown in the diagram of Fig. 2.4.1. To cancel the load current harmonics fed to the supply is the main purpose of the system. It can also contribute to reactive-power compensation and to balance three-phase currents. Parallel filters are more advantageous because it can carry the compensation current plus a small amount of current to reduce the system losses. It is also compatible with circuit suitable for a wide range of power ratings. This configuration consists of four categories of circuit, which are inverter configurations, lattice-structured filters, switched-capacitor circuits and voltage-regulator-type filters.

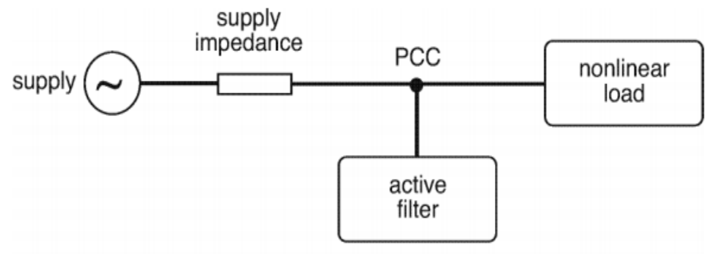

Figure 2.4.1: Parallel active filter configuration [92].

2.2.5.2 Series active power filters

The series active filter maintains a pure sinusoidal voltage waveform across the load by producing a PWM voltage waveform which is added/subtracted on an instantaneous basis, to/from the supply voltage [90, 93]. The main circuit configuration is shown in Fig. 2.4.2. The inverter configuration consist a system of a voltage-fed inverter not having any current-control loops. Series active filters are less used industrially than parallel active filters. This drawback in the system is because of series circuits, as it has to handle high load currents, which increases their current rating compared with parallel filters, mainly in the secondary side of the coupling transformer. The main advantage of series filters over parallel filters is that they have ability to eliminate voltage-waveform harmonics, and can balance three-phase voltages [93-96]. It provides a pure sinusoidal waveform to the load, which is mainly important for voltage-sensitive devices such as superconductive magnetic-energy storage and power system-protection devices.

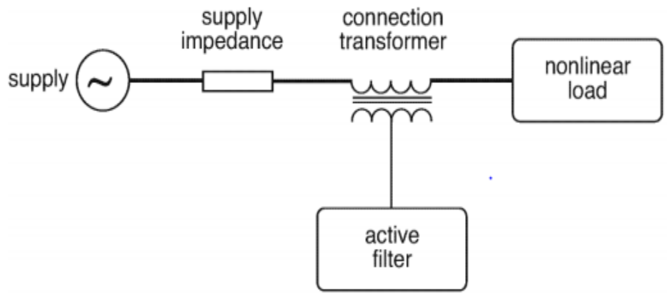

Figure 2.4.2: Series active filter configuration [92].

2.2.5.3 Combination of both parallel and series active filters

Combination of both series and parallel active filters provide an advantage over the individual active filter configurations, a combination of both types of filter is shown in Fig. 2.5.3. The demand for combined filters is limited as they have control complexity and higher cost. Because of their complexity and higher cost it has received less attention than other configurations [84, 85, 90, 97]. The arrangement is, however, frequently used for other purposes in power systems for flexible AC transmission systems [98].

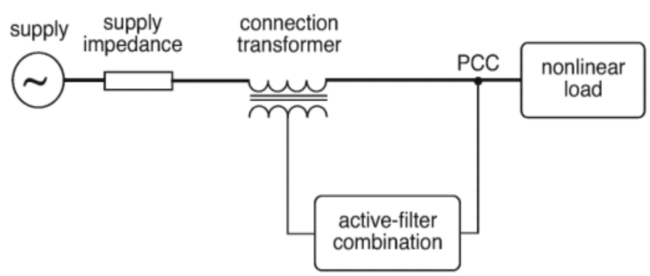

Figure 2.4.3: Combination of parallel and series active filters [92].

2.2.6 Superconducting magnetic energy storage (SMES)

SMES is a method of energy storage based on the fact that a current will continue to flow in a superconductor even after the voltage across it has been removed. SMES can simultaneously control the real and reactive power of the system to improve the system stability and power quality of a transmission grid [99-101]. A SMES system uses a magnet which is charged with external voltage supply. A SMES system may use number of magnets to store the energy but use of a lot of small magnets are more likely to be less economical than the single large magnet [102]. The energy stored is in a region well outside the magnet itself, but the magnetic stray field is to be shielded. To store the energy, we apply an amount of voltage and the magnetic field builds up until we reach the limit the magnet can stand. Whenever there is a decrease in the supply voltage power is drown from the SMES and the stored energy decreases exponentially. So, the SMES is capable of converting a decreasing steady voltage into the desired line voltage at 50 or 60 Hz. The main drawback is that it requires energy to be cooled.

Even though in some cases flicker cannot be completely mitigated, some solutions are implemented at the load level to lessen the occurrence and damage. They can be:

- Use of electronic fluorescent lamps which are less sensitive to voltage sags and replacing incandescent lights.
- Installing an uninterruptible power supply (UPS) and it is a very cost-effective solution if loads are subjected to disturbances which are identified and grouped together.
- Modification of the device which is generating the disturbance in the system. For example, use soft starters which reduce the starting current on motors which have to start frequently.

For limiting the amplitude of the voltage fluctuations some other mitigation measures are focused below:

- Modifying the network to increase the short-circuit current capacity on lighting circuits which may be done by connecting them as close as possible to the power supply point.

- Increasing the "electrical distance" between the disturbing loads and between the lighting circuits by using an independent transformer for powering the disturbing loads.
- Providing real time capacitive reactive compensation for each phase by using reactive compensation.
- For reducing the inrush current and smoothing the peak current demand a connection of a series inductance on the disturbing load.

However, if the flicker problem is occurring on the utility, there is one method adopted and that is to increase the short circuit capacity of the utility. This could be achieved by:

- Connecting the loads which are offending at a higher voltage level on the utility;
- Using a dedicated utility supply for the offending loads;
- Using separate distribution transformers to separate offending loads from other loads;
- Increasing the supply transformer kVA capacity or decreasing its impedance.

Chapter 3: Proposed Technique using EKF

As we had followed Kalman filter estimation technique a brief description of Kalman filter and its basic algorithm is shown in section 3.1 and 3.2 respectively. We had shown two types of Kalman filter- the discrete and extended Kalman filter in section 3.3 and 3.4. Enhanced phase-locked loop is described in 3.5. In this chapter we have demonstrated the use of PLL where the phase and frequency variables had been combined and the envelope of the grid voltage has been extracted using EPLL in section 3.6. The estimation of the grid voltage fundamental instantaneous flicker level (IFL) and actual fundamental voltage amplitude using the EKF technique has been described in section 3.7.

3.1 Kalman Filter

The Kalman filter is a set of mathematical equations that can help with the computational process to estimate the state of the process in an efficient way. It is useful because it supports and takes into account the past and present state of the process to predict future states even if the precise nature of the modeled system is unknown [74, 103]. A simple diagram explaining the continuous process of a Kalman filter is given below Figure3.1.

The algorithm used for the Kalman filter works in a two-step process. In the prediction step, the Kalman filter produces estimates of the current state variables, along with their uncertainties. Once the outcome of the next measurement is taken, these estimates are updated using a weighted average, with more weight being given to estimates with higher certainty. This process is computational. It can be done using only the present input measurements (k) and the previously (k-1) calculated state and its uncertainty matrix. No further steps are required to estimate the next state other than the present state (k) and previous state (k-1) [74].

The measurements taken from the initial prediction state usually contains some form of error or noise that is neutralized through continuous update and time and measurement updates.

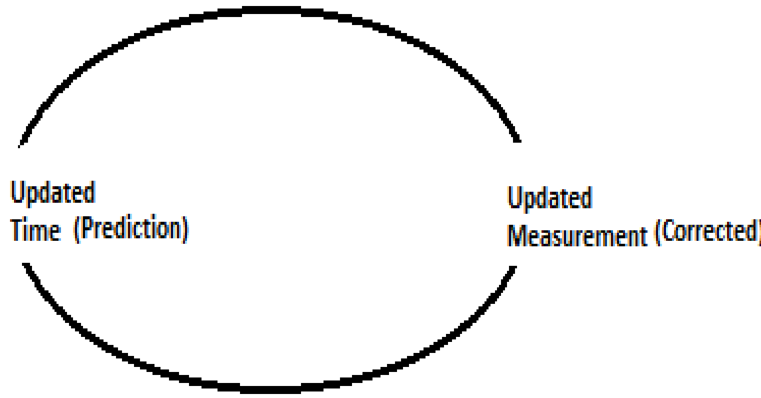

Figure 3.1: The Kalman filter update cycle.

3.2 Basic Algorithm of the Kalman Filter

The Kalman filter requires the previous state estimates $\hat{x}_k^-$ and the present state estimates x_k at state k-1 and k respectively. The measurement at state k is z_k. The present and previous state errors can be found out by the following equations [104-108]

$$e_k^- = x_k - \hat{x}_k^- \quad ;$$

$$e_k = x_k - \hat{x}_k$$

The previous state and present state error covariance's can be written as-

$$P_k^- = E[e_k^- e_k^{-T}] \quad ;$$

$$P_k = E[e_k e_k^T]$$

Here the operator 'E' denotes the mean value of its argument.

The next step is to find an equation that computes latter state $\hat{x}_k$ by taking into account the linear difference of previous state estimate $\hat{x}_k^-$ and the difference between the actual measurement of step k that is z_k and a weighted difference of $H\hat{x}_k^-$. The operator 'H' denotes the weight that has been introduced to neutralize the error from each step. So, the equation stands like this,

$$\hat{x}_k = \hat{x}_k^- + K(z_k - H\hat{x}_k^-)$$

If the difference $z_k - H\hat{x}_k^-= 0$ then both the states are equal. $z_k - H\hat{x}_k^-$ is also known as residual. K is said to be the Kalman gain. It has to set in such a way that the overall error from P_k can be reduced. A few steps are required to get the value of K. First we need to substitute the value of $\hat{x}_k$ to e_k. Then the new value of e_k needs to be put into P_k. After that taking the derivative of the result with respect to K and then solving that equation for zero will result in a value of K. A form that has been calculated from P_k can be written as [105, 108]-

$$K_k = \frac{P_k^- H^T}{HP_k^- H^T + R}$$

From the equation we can say that if the measurement error covariance approaches zero then the K weights the residual more heavily and if the error covariance of the previous state P_k^- approaches zero then the residual is weighted lightly [74].

3.3 Discrete Kalman Filter

In this form both Time and Measurement is being updated. So, there will be equations to update both the parameters. They are given below [74]-

Time update equations are as follows-

$$\hat{x}_k^- = A\hat{x}_{k-1} + Bu_{k-1} \;;$$

$$P_k^- = AP_{k-1}A^T + Q$$

'Q' is the noise covariance. The first equation comes from the linear stochastic difference equation.

Measurement update equations are as follows [74]-

$$K_k = \frac{P_k^- H^T}{HP_k^- H^T + R} \;;$$

$$\hat{x}_k = \hat{x}_k^- + K(z_k - H\hat{x}_k^-);$$

$$P_k = (I - K_k H)P_k^-$$

The first step is to calculate the Kalman gain K_k. Then the actual measurement z_k is calculated to find out $\hat{x}_k$. The final step is to obtain a present error covariance estimate from P_k. In the last measurement update equation 'I' is used as an identity matrix [74].

A sequence showing how the discrete Kalman filter works is given below. Where each parameter has their distinct meaning-

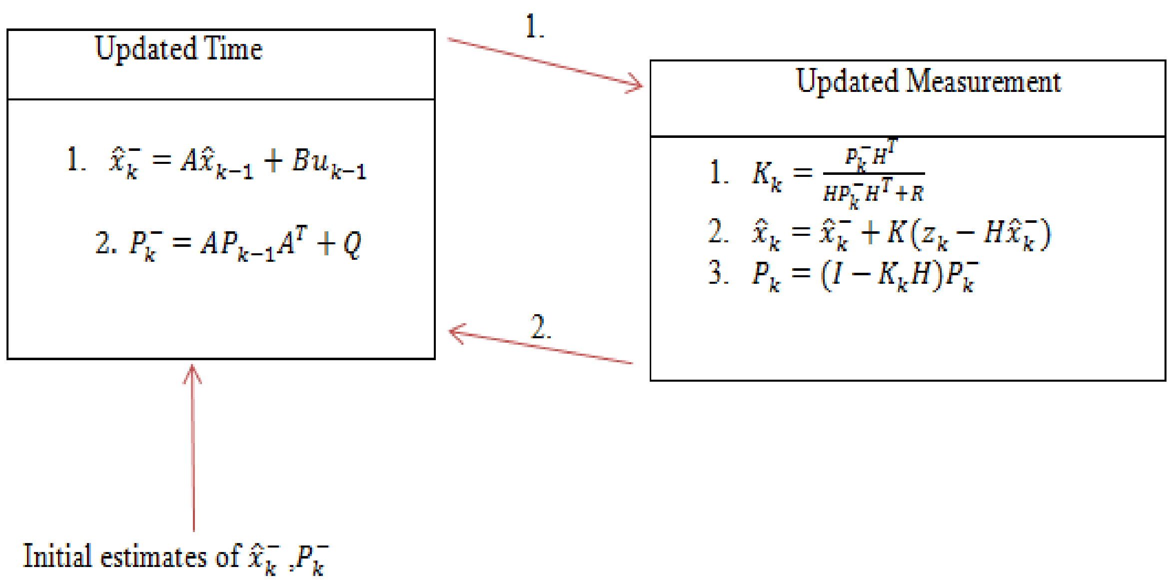

Figure 3.2: Sequence showing how a discrete Kalman Filter operates.

3.4 Extended Kalman Filter

A Kalman filter that linearizes about the current mean and covariance is referred to as an extended Kalman filter or EKF. In discrete Kalman filter we used linear stochastic difference equation but since we are using EKF and the problem is non-linear we will use non-linear stochastic difference equation. The equation is as follows [74]-

$$x_k = f(x_{k-1}, u_{k-1}, w_{k-1})$$

And the measurement follows the equation-

$$z_k = h(x_k, v_k)$$

Here w_k and v_k are the process and process and measurement noise.

In practical application w_k and v_k can't be known for all the states. Approximate state and measurement vectors can be calculated without them [74, 109]-

$$\tilde{x}_k = f(\hat{x}_{k-1}, u_{k-1}, 0);\ \tilde{z}_k = h(\tilde{x}_k, 0)$$

We need two equations that can linearize the equations given above [74]-

$$x_k \approx \tilde{x}_k + A(x_{k-1} - \hat{x}_{k-1}) + Ww_k$$

$$z_k \approx \tilde{z}_k + H(x_k - \tilde{x}_k) + Vv_k$$

These two equations have been developed to help linearize a non-linear equation. Here, x_k and z_k are the actual measurements, $\tilde{x}_k$ and $\tilde{z}_k$ are approximate measurements, w_k and v_k are the process and process and measurement noise.

Measurement error and residual is given by the following equations-

$$\tilde{e}_{x_k \equiv x_k - \tilde{x}_k}$$

$$\tilde{e}_{z_k \equiv z_k - \tilde{z}_k}$$

But still x_k and z_k are not available in practical condition as they are the actual measurements instead the equations can written as [74]-

$$\tilde{e}_{x_k} \approx A(x_{k-1} - \hat{x}_{k-1}) + \mathcal{E}_k$$

$$\tilde{e}_{z_k} \approx H\tilde{e}_{x_k} + \eta_k$$

Using these equations, we can make an equation to calculate the present state estimation for the original non-linear equation.

$$\hat{x}_k = \widetilde{x}_k + \widehat{e}_k$$

Here,$\hat{e}_k$ is calculated from $\tilde{e}_{z_k \equiv z_k - \tilde{z}_k}$ & $\tilde{e}_{x_k} \approx A(x_{k-1} - \hat{x}_{k-1}) + \mathcal{E}_k$.

Assuming that the predicted value of $\hat{e}_k$ is zero, the Kalman filter equation used to estimate $\hat{e}_k$ is [74]-

$$\hat{e}_{k=}K_k\tilde{e}_{z_k}$$

Now using this in equation $\hat{x}_k = \widetilde{x}_k + \widehat{e}_k$ and replacing $\tilde{e}_{z_k}$ with $\tilde{e}_{z_k \equiv z_k - \tilde{z}_k}$. We get-

$$\hat{x}_k = \widetilde{x}_k + K_k(z_k - \tilde{z}_k)$$

This equation can now be used in the calculation of measurement update in the EKF. We will get $\tilde{x}_k$ and $\tilde{z}_k$ from $x_k = f(x_{k-1}, u_{k-1}, w_{k-1})$ and $z_k = h(x_k, v_k)$ respectively. K_k will come from $K_k = \frac{P_k^- H^T}{HP_k^- H^T + R}$ [103, 108]. Finally, the time and measurement update equations can be written.

Time update equations are as follows [74]-

$$\tilde{x}_k^- = f(\hat{x}_{k-1}, u_{k-1}, 0)$$

$$P_k^- = A_k P_{k-1} A_k^T + W_k Q_{k-1} W_k^T$$

Here, A_k and W_k are the process Jacobians and Q_k is the process noise covariance.

Measurement update equations are as follows [74]-

$$K_k = P_k^- H_k^T / (H_k P_k^- H_k^T + V_k R_k V_k^T)$$

$$\hat{x}_k = \hat{x}_k^- + K_k(z_k - h(\hat{x}_k^-, 0))$$

$$P_k = (I - K_k H_k) P_k^-$$

The sequence diagram of the EKF can be drawn from this equation-

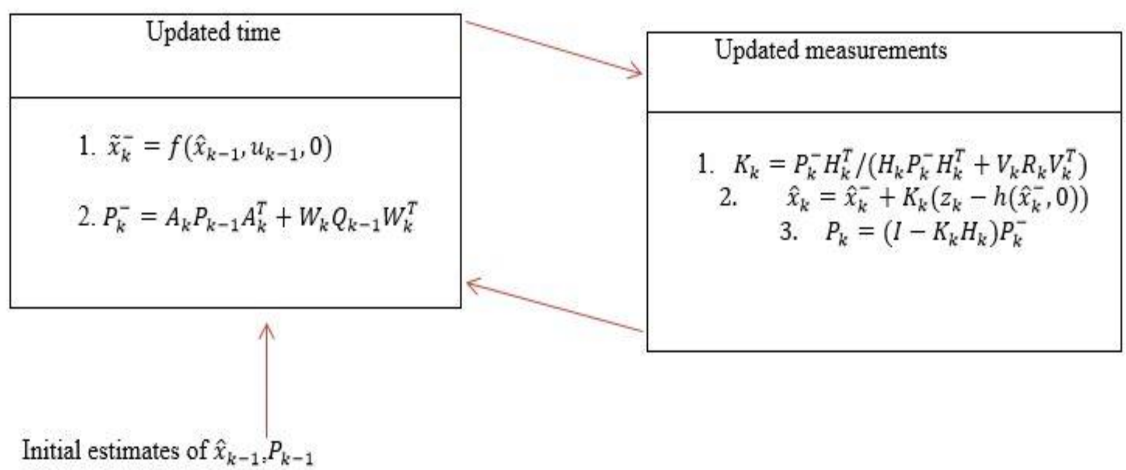

Figure 3.3: Sequence showing how an Extended Kalman Filter operates.

3.5 Enhanced Phase-Locked Loop (EPLL)

The EPLL or the enhanced PLL is known by its task to estimating the amplitude of a desired input signal which can be further used in a new loop to remove errors. The enhanced phase-locked loop removes the main drawback the double frequency errors of the simple standard PLL and thus enhances it. The EPLL provides a filtered version of the input signal, it provides and estimation of the input signal magnitude and removes the ripples. So, the EPLL is mainly working as a filter for the input signal.

The block diagram of the EPLL is shown in Figure 3.4. It was first introduced in this format with minor differences of presentation in References [110].

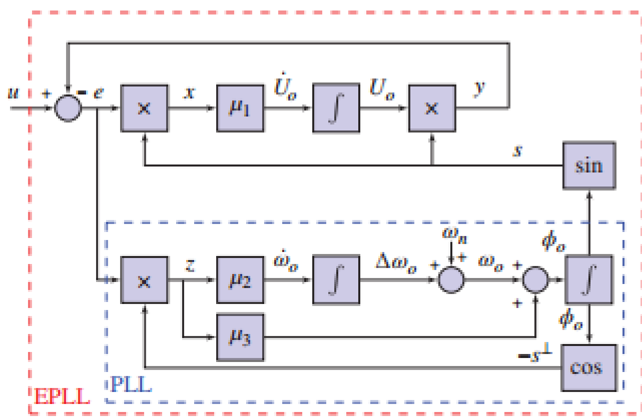

Figure 3.4: Block diagram of the EPLL [111].

The EPLL generally contains a PLL (shown in the figure), it gives a filtered version of the input signal *u*, which is demonstrated by the following equation $y = U_0 sin\emptyset_0$. Here, $\emptyset_0$ is the phase angle of the input signal and the peak amplitude of the input signal is derived by U_0. ω_0 estimates the frequency of the signal. There is a unity sinusoidal signal *s* which is in phase with the input signal *u*, a stability in the synchronization is thus obtained. There is a signal $s^{\perp}$ which is in 90◦ phase-delay with *s*. So, the signal $y^{\perp}$ can be described by $y^{\perp} = U_0 s^{\perp}$. The performance of EPLL is controlled by the constants $\mu 1$, $\mu 2$, and $\mu 3$. The following signals can be generated by the EPLL [112];

1. Estimated phase angle: $\emptyset_0$
2. Estimated frequency: ω_0

3. Estimated rate of change of frequency: $\omega^{\cdot}$
4. Estimated amplitude: U_0
5. Estimated rate of change of amplitude: $U^{\cdot}{}_0$
6. Normalized synchronizing signal: *s*
7. Normalized quadrature (90◦ phase-delayed) signal: $s^{\perp}$
8. Estimated fundamental component: *y*
9. Estimated quadrature of fundamental component: $y^{\perp} = U_0 s^{\perp}$
10. Distortions and noise: *e*

The EPLL has three gain values: *μ1, μ2,* and *μ3* which are adjustable. The parameters can be adjusted by the following methods [112-114].

• Let $\mu = 2\zeta_1\omega_n$. Where ω_n= the nominal value of input frequency,

And ζ_1= the first damping ratio.

Choosing the value of ζ_1 we can calculate *μ*, then we can calculate *μ1 =μ3 =μ*.

• Let $2\zeta_2\omega_r = \frac{\mu}{2} = \zeta_1\omega_n$. Where ζ_2= the second damping ratio,

and ω_r=the bandwidth corresponding to the phase/frequency linear loop.

Choose the value of ζ_2 we can calculate *μ2*, from $\omega_r^2 = \frac{\mu 2}{2}$.

3.6 Extraction of envelope using EPLL

In this Simulation the EPLL is used for its advantage of giving stable synchronizing signal (with unity magnitude) at the VCO output. In this Paper, we have demonstrated an adaptive strategy to address the probability of flicker. This method is based upon frequently adjusting the frequency estimation loop gain in order to lessen the false frequency transients at the instant of phase angle jumps and also in the startup stage [115].

In this case we had taken the input grid voltage equation as follows;

$$u = (A + AF * \sin(2 * \pi * fF * k * Ts)) * \sin(2 * \pi * f * k * Ts) \qquad (1)$$

Where each parameter have their individual meaning. We had taken a Fundamental component of y where;

$$y = A * sin(\varphi)$$

Here Ts = sampling time, k = the sampling instant, f = fundamental frequency of grid voltage, A = fundamental Voltage amplitude, AF = Flicker amplitude, fF = Flicker frequency.

We had set the values of the Parameters as follows; fF = 5, A = 1, f = 50Hz, Ts = 0.00025(sampling frequency fs = 4kHz). We have shown two cycles of simulations where k = 1-8000. The φ is known as the phase angle. Where;

$$\varphi \; = \; 2\pi fkTs + \theta$$

Here, θ = initial phase angle of the voltage flicker. We had set the initial value of θ as $\theta =$ 0.

In the procedure for extracting the grid voltage flicker we had set the differential equations of the EPLL as (A, ω, φ) amplitude, frequency, and phase angle respectively [115]. Here;

$$A^{\cdot} \; = \; \mu 1 \; e \; sin\varphi \qquad (2)$$

$$\Delta \, \omega^{\cdot} \; = \; \mu 2 \; e \; cos\varphi$$

$$\varphi^{\cdot} \; = \; \omega o \; + \; \Delta\omega \; + \; \mu 3 \; e \; cos\varphi$$

Where the grid voltage nominal frequency is $\omega o = 2\pi f$. We had defined e as the error signal where e = u-y. Both e and $\mu 1$, $\mu 2$, $\mu 3$ are EPLL gains and they are both positive numbers. We had defined $\mu 1$, $\mu 2$, $\mu 3$ as [112, 115];

$$\mu 1 = \mu 3 = \mu = P * \omega o$$

$$\mu 2 = \frac{\mu^2}{8}$$

Here we had set the value of P as $P = \sqrt{2}$, because the larger value of $P = 0.5 \leq P \leq 1.5$ had given us faster response with larger oscillations [115].

In the next section we are constantly updating the value of Input grid voltage u. In the event of simulation, we had taken the sampling interval from 1-8000. The input grid voltage is as follows-

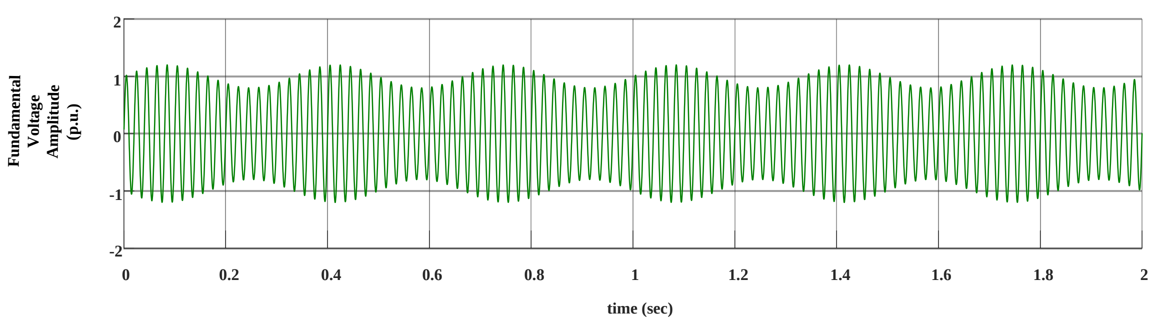

Figure 3.5: Waveform of input Grid Voltage at EPLL input.

By constantly updating the values of phase angle φ , frequency $\Delta\omega$, and the error signal e we had got the desired output of the envelope of the grid voltage amplitude by which we may estimate the instantaneous flicker level present in the system. The output of the simulation is shown below-

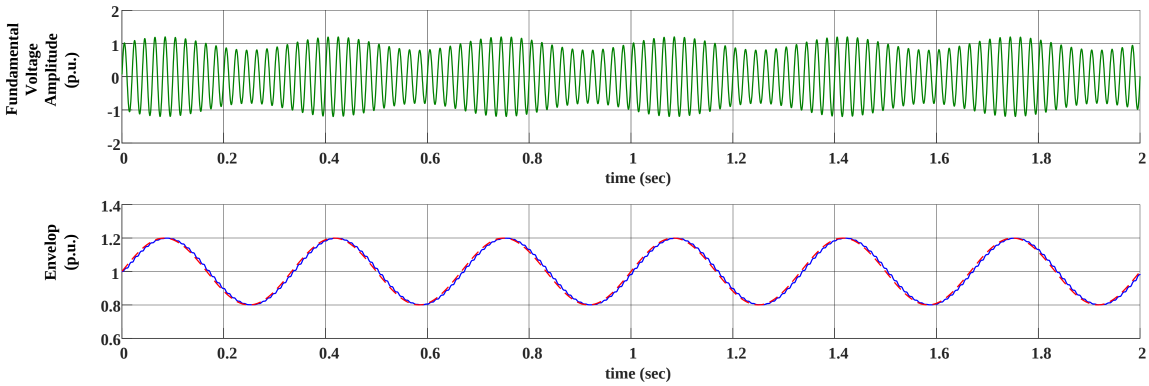

Figure 3.6: Output waveform of the envelope of grid voltage.

3.7 Estimation of voltage flicker through extended Kalman filter technique

It has been assumed that in the grid voltage waveform as given in Figure 3.5 suffers from flicker. We have used the EKF technique for the purpose of flicker estimation [22, 36, 116-118]. The inputs of the EKF are the harmonics component (flicker amplitude, frequency and phase) which are estimated from (2) of the grid voltage waveform in section 3.6. The general expression of EKF input at the *k*th sampling instant can be expressed by;

$$A^{\cdot} = A + \mu 1\, e\, sin\varphi$$

Where, A = fundamental Voltage amplitude.

Let us consider that the states of the in-phase and the in-quadrature components of the harmonic at the kth sampling instant for instantaneous flicker parameters estimation are given by x1F(k), x2F(k), x3F(k) and x4F(k) respectively [117, 118]. Where,

$$x1F(k) = AF(k) * sin(\varphi(k))$$

$$x2F(k) = AF(k) * cos(\varphi(k))$$

$$x3F(k) = fF(k)$$

$$x4F(k) = A(k)$$

And;

$$\varphi = 2 * \pi * fF(k) * Ts + \theta$$

Where, θ = initial phase angle of the voltage flicker. We had set the initial value of θ as $\theta = 0$. The amplitude of voltage flicker AF(k) = 0.2 , the initial instantaneous phase angle of voltage flicker $\varphi(k)$ = 0.0101, fundamental voltage amplitude A(k) = 1, frequency of voltage flicker $fF = 5Hz$.

The estimation of the instantaneous time-varying grid voltage flicker with the use of EKF is based on the fact that the phasor is rotated by the amount of $2 * \pi * fF(k) * Ts$ at the $(k+1)^{th}$ state [118].

Here, the $x1F(k)$ state expresses the IFL present in the waveform of grid voltage. The actual amplitude of fundamental voltage waveform and the flicker frequency are obtained directly from the states $x4F(k)$ and $x3F(k)$ respectively.

Here, the instantaneous amplitude and the phase angle of the harmonic component can be updated at the kth instant by $AF(k)$ and φ respectively [118]. Where,

$$AF = \sqrt{(x1F(k))^2 + (x2F(k))^2}$$

$$\varphi = \arctan\left\{\frac{x1F(k)}{x2F(k)}\right\}$$

In the event of simulation, we had taken the sampling interval (k) from 1-8000.

The state vectors at the kth sampling time instant, state transition matrix *DF* and measurement matrix *HF* of the EKF can also be expressed by (3), (4), (5), and (6) respectively. Where;

$$xF = [x1F(k);\ x2F(k);\ x3F(k);\ x4F(k)]$$

$$DF = \begin{bmatrix} \cos(2*\mathrm{pi}*\mathrm{x3F(k)}*\mathrm{Ts}) & \sin(2*\mathrm{pi}*\mathrm{x3F(k)}*\mathrm{Ts}) & 0 & 0 \\ -\sin(2*\mathrm{pi}*\mathrm{x3F(k)}*\mathrm{Ts}) & \cos(2*\mathrm{pi}*\mathrm{x3F(k)}*\mathrm{Ts}) & 0 & 0 \\ 0 & 0 & 1 & 0 \\ 0 & 0 & 0 & 1 \end{bmatrix}$$

$$HF = [cos(2*pi*x3F(k)*Ts) \quad sin(2*pi*x3F(k)*Ts) \quad 0 \quad 1\ ]$$

Where;

$$DF(1,3) = 2*pi*Ts*[-x1F(k)*sin(2*pi*x3F(k)*Ts) + x2F(k)*cos(2*pi*x3F(k)*Ts)]$$

$$DF(2,3) = 2*pi*Ts*[-x1F(k)*\cos(2*pi*x3F(k)*Ts) - x2F(k)*\sin(2*pi*x3F(k)*Ts)\ ]$$

$$HF(1,3) = 2*pi*Ts*[-x1F(k)*\sin(2*pi*x3F(k)*Ts) + x2F(k)*\cos(2*pi*x3F(k)*Ts)\ ]$$

The steps of the EKF algorithm are given below for each sampling instant [118]:

- Time update stage-

1. Projecting the state ahead by; $xF(k) = DF * xF(k-1)$
2. Projecting the error covariance ahead: $P(k) = DF * P(k-1) * (DF)^T + Q$

- Measurement update stage-

1. The Kalman gain is updated by:

$$K = P(k) * (HF)^T * (HF * P(k) * (HF)^T + R)^{-1}$$

2. Estimation of the update of state expression of EKF after the time update stage:

$$xF(k+1) = xF(k) + K * (A^{\cdot} - HF * xF(k))$$

Where, The general expression of EKF's input at the kth sampling instant can be expressed by $A^{\cdot}$. T denotes the transpose operation.

3. Update of the error covariance after the time update stage:

$$P(k+1) = (I - K * HF) * P(k)$$

Where, P, Q, K, R and I are the error covariance matrix, process noise covariance matrix, Kalman filter gain, measurement noise and the identity matrix respectively.

We had updated the states of the EKF at each sampling instant for next stage for instantaneous flicker parameters estimation and for $(k+1)^{th}$ sampling instant. The states may be denoted by the following equations –

$$x1F(k+1) = xF(1)$$

$$x2F(k+1) = xF(2)$$

$$x3F(k+1) = xF(3)$$

$$x4F(k+1) = xF(4)$$

By plotting the equation of *x1F* we had got the EKF output for the IFL present in the grid voltage waveform.

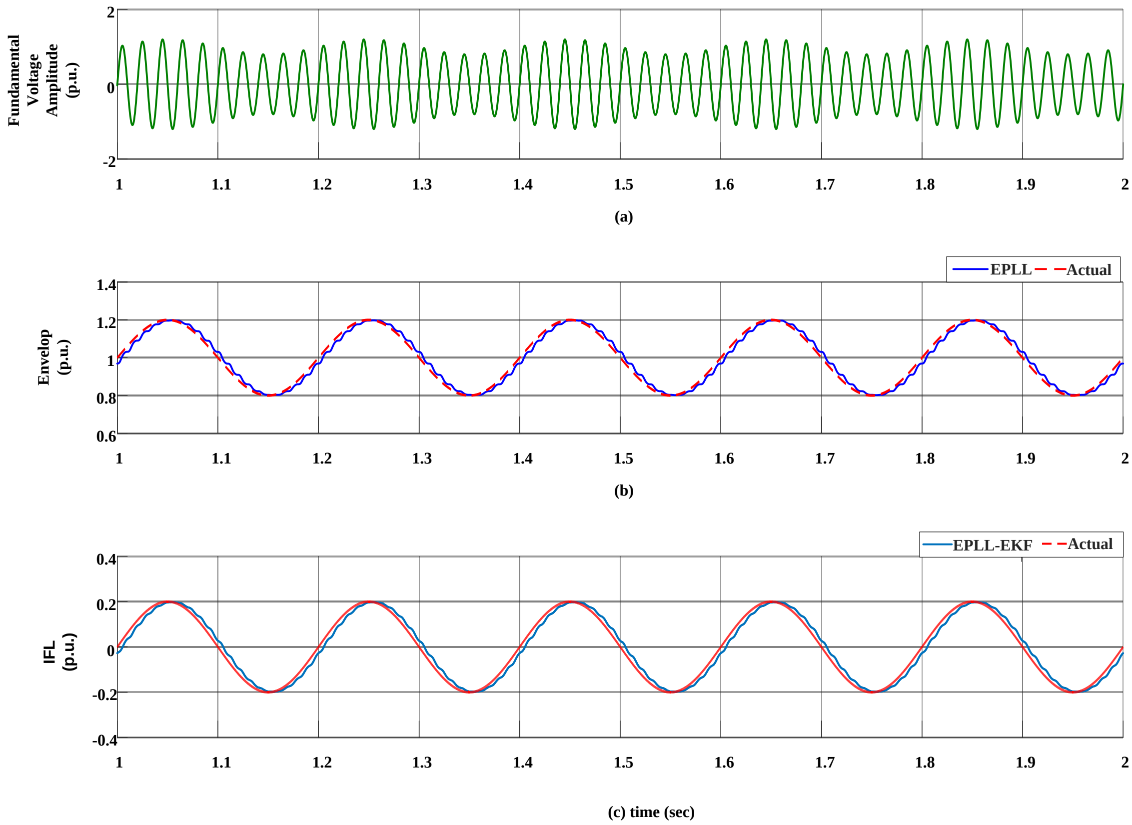

Figure 3.7: EKF output waveform for the IFL present in the grid voltage.

Chapter 4: Simulation Results

In this chapter the simulation results for the proposed technique of flicker estimation applying Enhanced phase locked loop (EPLL) and Extended Kalman Filter (EKF) has been presented. Section 4.1 describes the environment of the simulation process. Simulations illustrating the tracking capability of EKF for sinusoidal flicker with constant grid voltage has been provided in section 4.2. Section 4.3 provides the simulation results illustrating the performance of the EPLL for different flicker waveforms. In section 4.4 simulations combining EPLL and EKF to extract the flicker directly from grid voltage has been presented.

4.1 Simulation Environment

In order to demonstrate the performance of the proposed technique, numerous simulations are performed in MATLAB environment. The amplitudes of all the voltage components are considered as p.u. basis. 4 kHz and 50 Hz are chosen as the sampling frequency and nominal grid fundamental frequency, respectively.

The simulations have been performed under the consideration that all signals are free of harmonics. To observe the flicker tracking capability of the proposed EPLL-EKF technique, the sinusoidal, triangular, saw tooth and the square variations of instantaneous flicker are applied to the grid voltage waveform. A periodic triangular variation of both Fundamental and flicker frequency is also applied to observe the time varying frequency tracking capability of the proposed technique.

4.2 Case-A: Estimation of Voltage flicker using EKF only

In this case a constant grid voltage of fundamental amplitude 1 p.u. is considered. A sinusoidal flicker AF*sin(2πf_Ft) is included in the grid voltage to observe the flicker tracking capability of EKF. The grid voltage with flicker (1+ AF*sin(2πf_Ft)) is shown in fig 4.1(a). Fig 4.2(b) shows the extracted flicker AF*sin(2πf_Ft) for 2 sec. Since the EKF predicts the next value from the existing data, initially a few milliseconds is required to start tracking accurately.

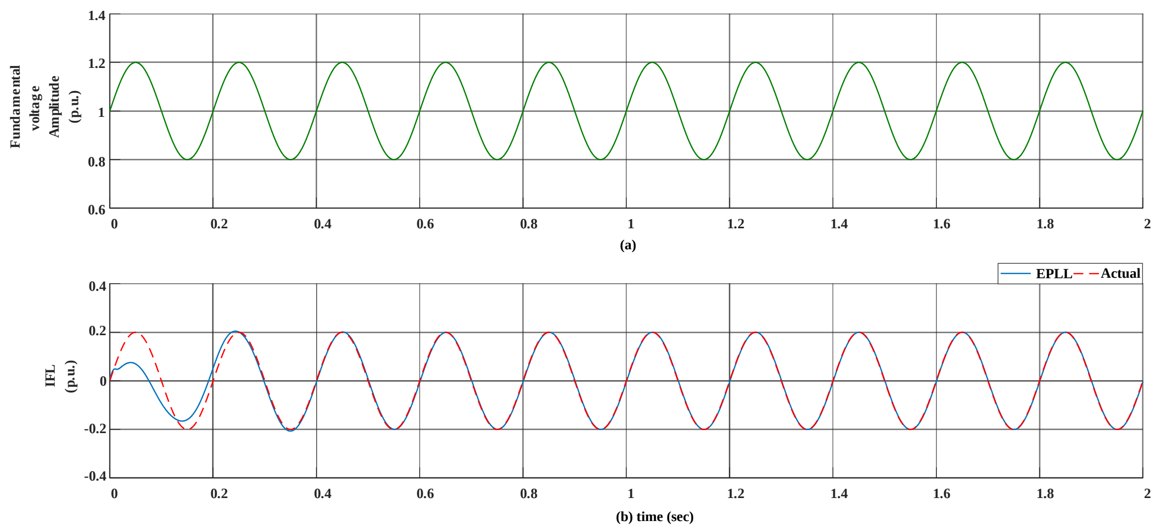

Figure 4.1: Estimation of Voltage flicker using EKF only, where AF = 0.2 p.u. and f_F = 5 Hz (a) Fundamental voltage amplitude. (b) Instantaneous flicker level (IFL).

4.3 Case-A: Extraction of amplitude (envelope) of grid voltage affected by flicker applying EPLL

4.3.1: Case-A1: Amplitude of grid voltage affected by sinusoidal flicker

In this case the grid voltage of fundamental frequency 50 Hz is suffering from a sinusoidal flicker of amplitude 0.2 p.u. and frequency 5 Hz as shown in fig 4.2 (a). An enhanced PLL is applied to extract the envelope of this voltage which contains the fundamental amplitude plus flicker as shown in fig 4.2 (c). Error signal is plotted as the difference of input and estimated voltage.

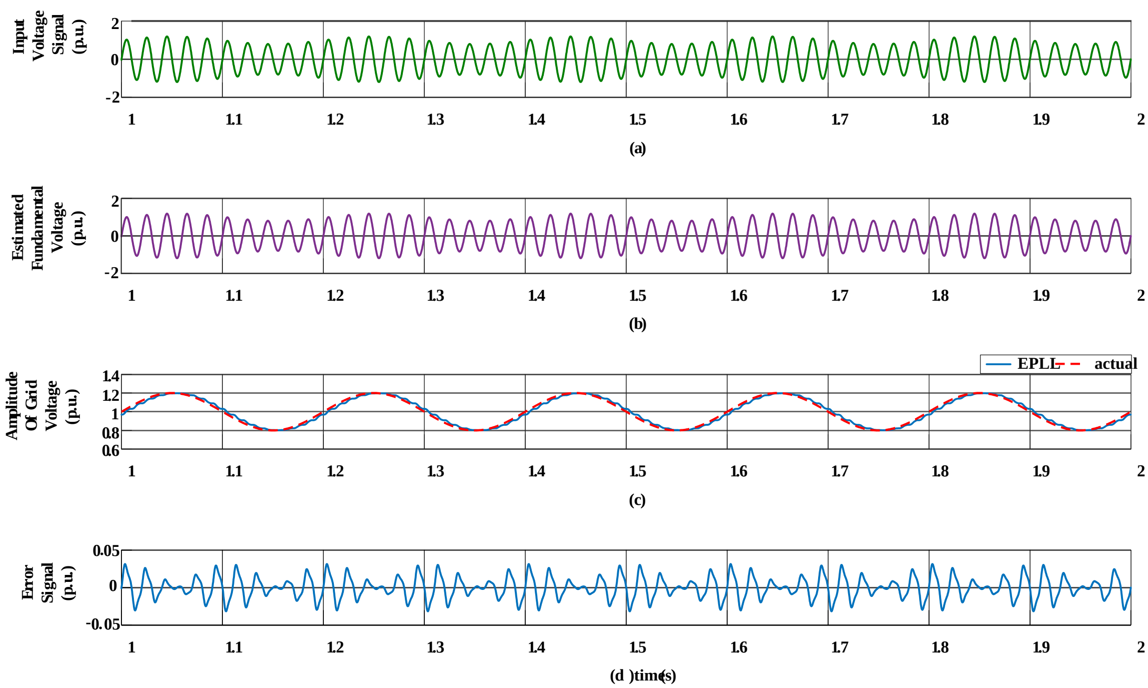

Figure 4.2: Extraction of amplitude of grid voltage affected by sinusoidal flicker applying EPLL, where AF = 0.2 p.u. and f_F = 5 Hz (a) Input Voltage Signal(p.u.) (b) Estimated Fundamental output voltage(p.u.) (c) Amplitude of grid voltage(p.u.) (d) Error signal(p.u.).

4.3.2: Case-A2: amplitude of grid voltage affected by triangular flicker

In this case the grid voltage of fundamental frequency 50 Hz is suffering from a triangular flicker of amplitude 0.2 p.u. and frequency 5 Hz as shown in fig 4.3 (a). An enhanced PLL is applied to extract the envelope of this voltage which contains the fundamental amplitude plus flicker as shown in fig 4.3 (c). Error signal is plotted as the difference of input and estimated voltage.

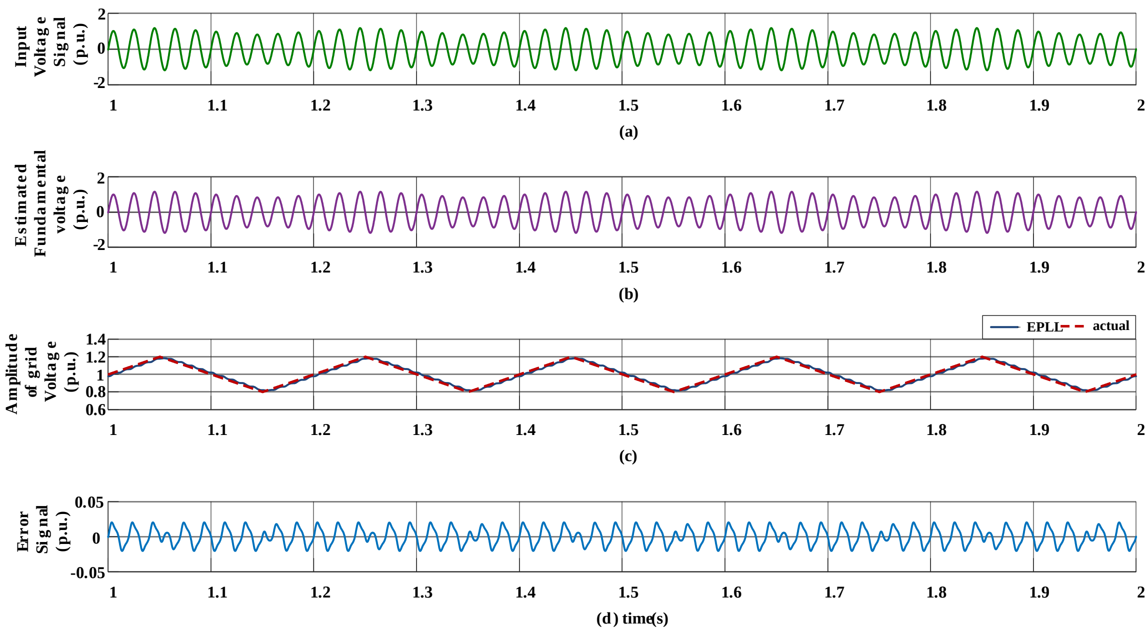

Figure 4.3: Extraction of amplitude of grid voltage affected by triangular flicker applying EPLL, where AF = 0.2 p.u. and f_F = 5 Hz (a) Input Voltage Signal(p.u.) (b) Estimated Fundamental output voltage(p.u.) (c) Amplitude of grid voltage(p.u.) (d) Error signal(p.u.).

4.3.3: Case-A3: amplitude of grid voltage affected by square flicker

In this case the grid voltage of fundamental frequency 50 Hz is suffering from a square flicker of amplitude 0.2 p.u. and frequency 5 Hz as shown in fig 4.4 (a). An enhanced PLL is applied to extract the envelope of this voltage which contains the fundamental amplitude plus flicker as shown in fig 4.4 (c). Error signal is plotted as the difference of input and estimated voltage.

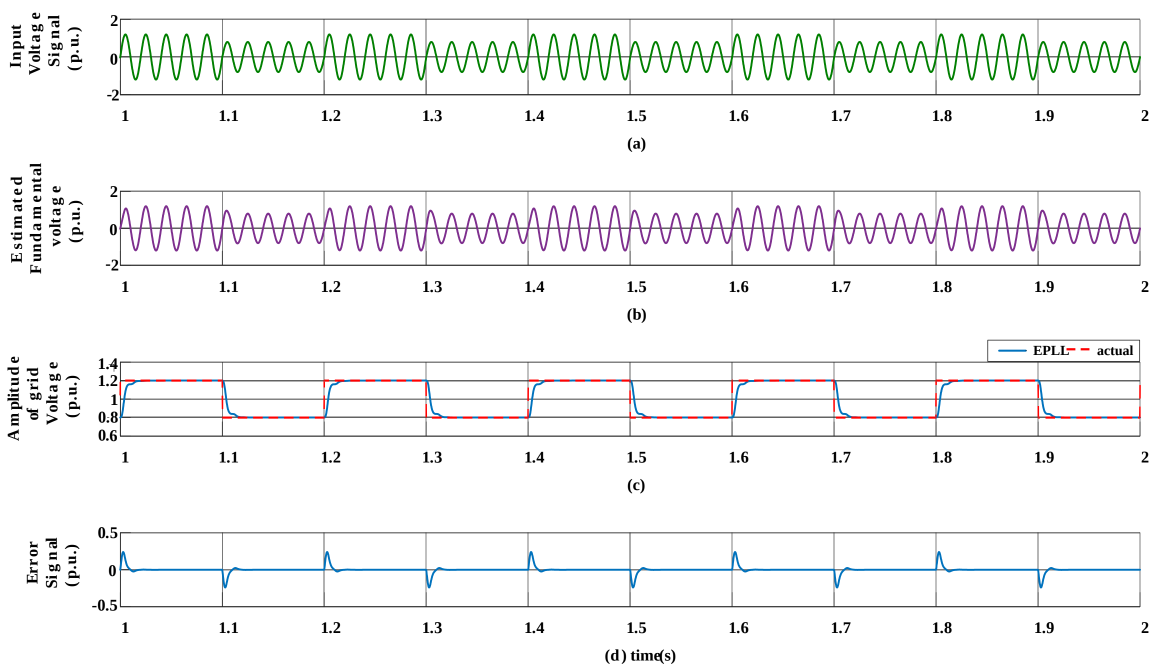

Figure 4.4: Extraction of amplitude of grid voltage affected by square flicker applying EPLL, where AF = 0.2 p.u. and f_F = 5 Hz (a) Input Voltage Signal(p.u.) (b) Estimated Fundamental output voltage(p.u.) (c) Amplitude of grid voltage(p.u.) (d) Error signal(p.u.).

4.3.4: Case-A4: amplitude of grid voltage affected by sawtooth flicker

In this case the grid voltage of fundamental frequency 50 Hz is suffering from a sawtooth flicker of amplitude 0.2 p.u. and frequency 5 Hz as shown in fig 4.5 (a). An enhanced PLL is applied to extract the envelope of this voltage which contains the fundamental amplitude plus flicker as shown in fig 4.5 (c). Error signal is plotted as the difference of input and estimated voltage.

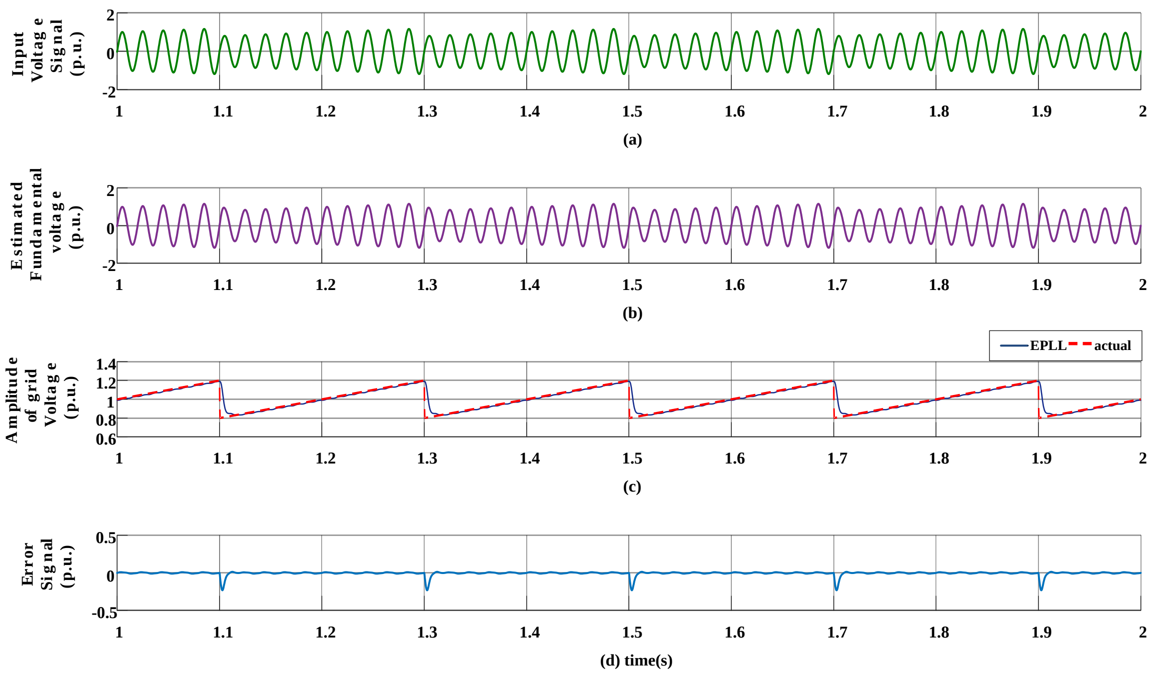

Figure 4.5: Extraction of amplitude of grid voltage affected by sawtooth flicker applying EPLL, where AF = 0.2 p.u. and f_F = 5 Hz (a) Input Voltage Signal(p.u.) (b) Estimated Fundamental output voltage(p.u.) (c) Amplitude of grid voltage(p.u.) (d) Error signal(p.u.).

4.3.5: Case-B1: Estimation of amplitude of grid voltage for a fundamental frequency rather than the nominal frequency

In this case a fundamental frequency(f) of 48 Hz is used instead of the nominal 50 Hz to test the performance of EPLL in a situation where grid voltage is subjected to any phase instability. The grid voltage also suffers from a sinusoidal flicker.

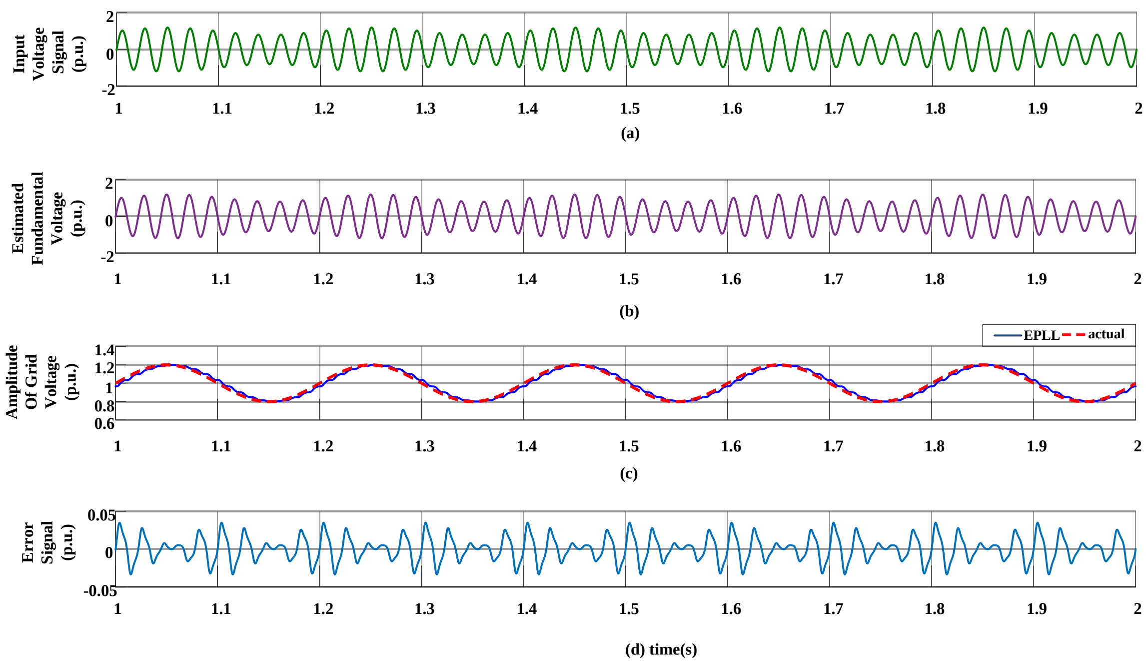

Figure 4.6: Estimation of amplitude of grid voltage for a fundamental frequency of 48 Hz applying EPLL, where AF = 0.2 p.u. and f_F = 5 Hz (a) Input Voltage Signal(p.u.) (b) Estimated Fundamental output voltage(p.u.) (c) Amplitude of grid voltage(p.u.) (d) Error signal(p.u.).

4.3.6: Case-B2: Estimation of amplitude of grid voltage for a fundamental frequency rather than the nominal frequency

In this case a fundamental frequency(f) of 52 Hz is used instead of the nominal 50 Hz to test the performance of EPLL in a situation where grid voltage is subjected to any phase instability. The grid voltage also suffers from a sinusoidal flicker.

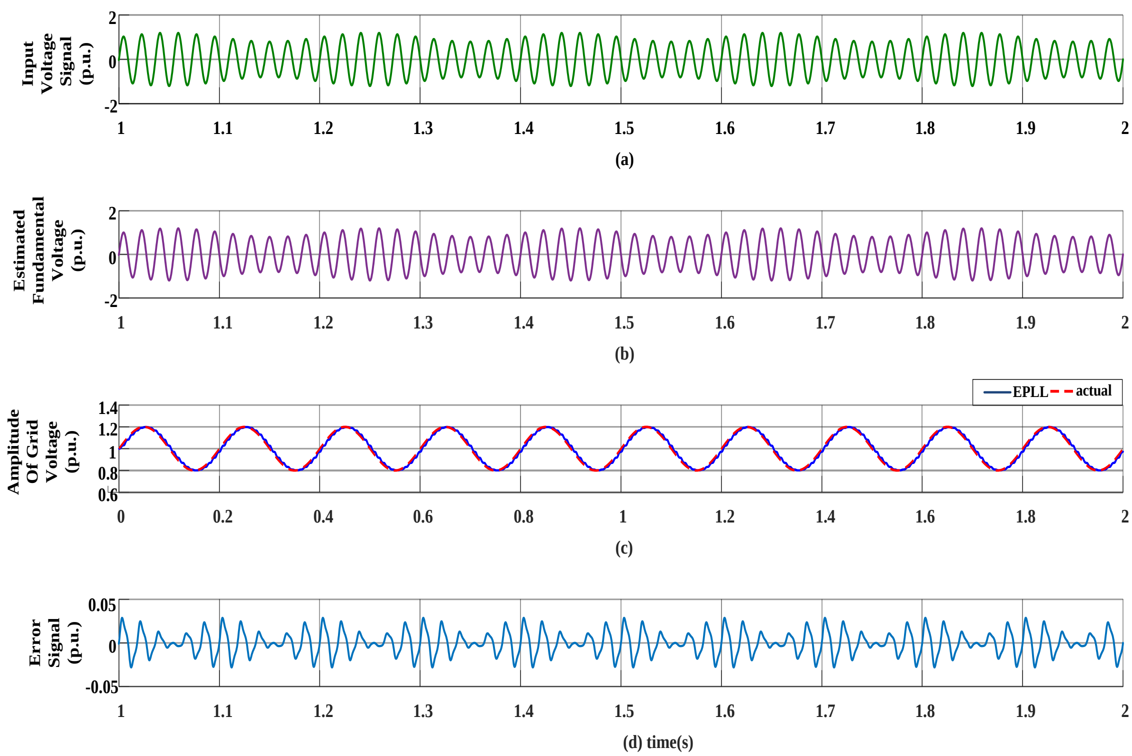

Figure 4.7: Estimation of amplitude of grid voltage for a fundamental frequency of 52 Hz applying EPLL, where AF = 0.2 p.u. and f_F = 5 Hz (a) Input Voltage Signal(p.u.) (b) Estimated Fundamental output voltage(p.u.) (c) Amplitude of grid voltage(p.u.) (d) Error signal(p.u.).

4.3.7: Case-B3: Estimation of amplitude of grid voltage in case of a variation of fundamental frequency rather than the constant nominal frequency

In this case the fundamental frequency is considered to be changing periodically rather than a constant value. It is varied linearly within 45 to 55 Hz in order to demonstrate the time varying frequency tracking capability of EPLL. It is observed that the system better tracks the amplitude when the fundamental frequency is high.

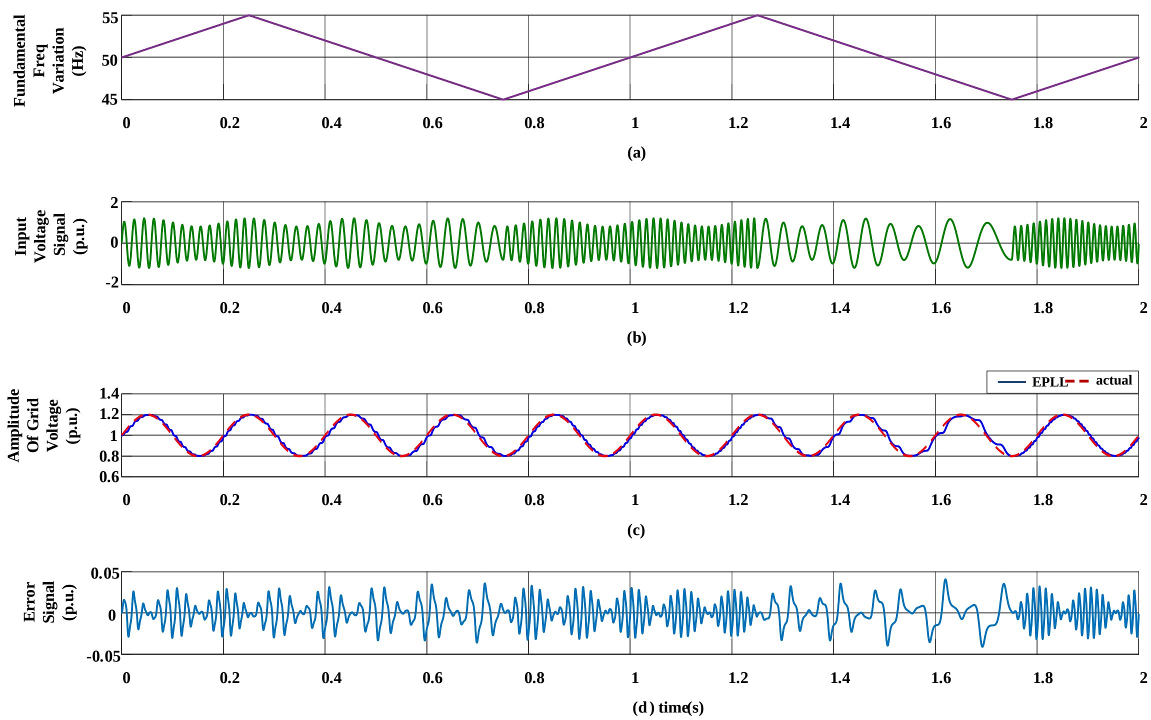

Figure 4.8: Estimation of amplitude of grid voltage for a fundamental frequency variation within 45-55 Hz applying EPLL, where AF = 0.2 p.u. and f_F = 5 Hz (a) Fundamental Frequency Variation(Hz) (b) Input Voltage Signal(p.u.) (c) Amplitude of grid voltage(p.u.) (d) Error signal(p.u.).

4.3.8: Case-C1: Estimation of amplitude of grid voltage in case of a variation of flicker frequency only

In this case the flicker frequency is varied from 2 Hz to 6 Hz in a triangular manner to reflect the practical scenario of flicker that its frequency is not constant. From fig 4.9(d) it is observed that the system better tracks the amplitude when the flicker frequency is low or decreasing.

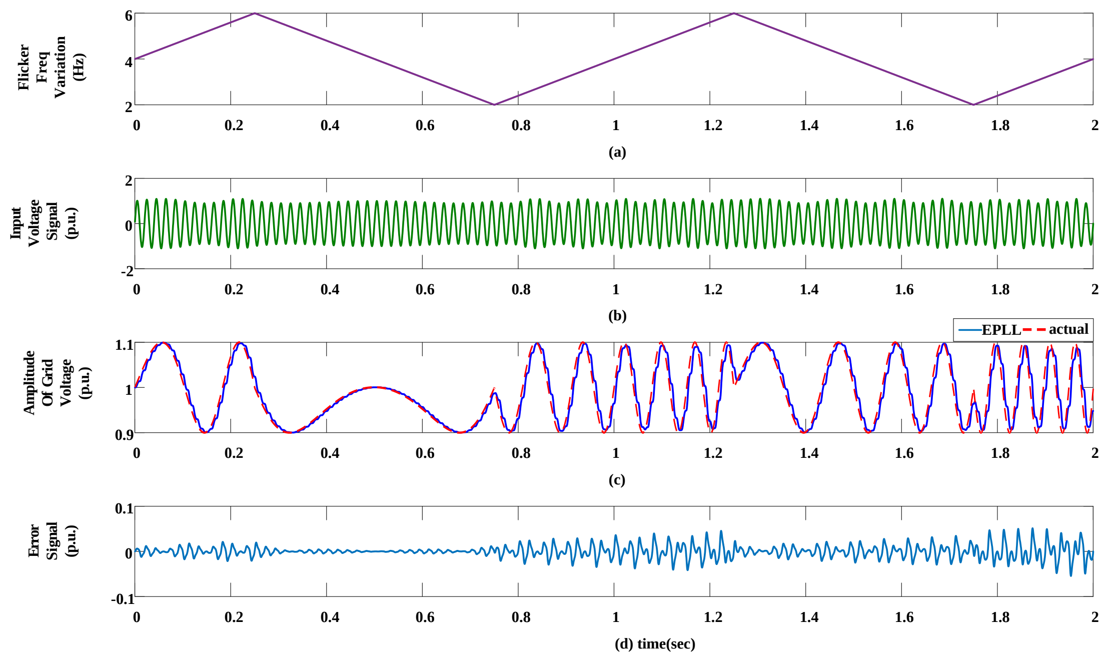

Figure 4.9: Estimation of amplitude of grid voltage for a flicker frequency variation within 2-6 Hz applying EPLL, where AF = 0.2 p.u. (a) Flicker Frequency Variation(Hz) (b) Input Voltage Signal(p.u.) (c) Amplitude of grid voltage(p.u.) (d) Error signal(p.u.).

4.3.9: Case-C2: Estimation of amplitude of grid voltage in case of a variation of flicker amplitude only

In this case the flicker amplitude is varied from -0.4 to 0.4 p.u. in a triangular manner to reflect the practical scenario of flicker that its amplitude is not constant. From fig 4.10(d) it is observed that the system better tracks the grid voltage amplitude when the flicker amplitude is zero.

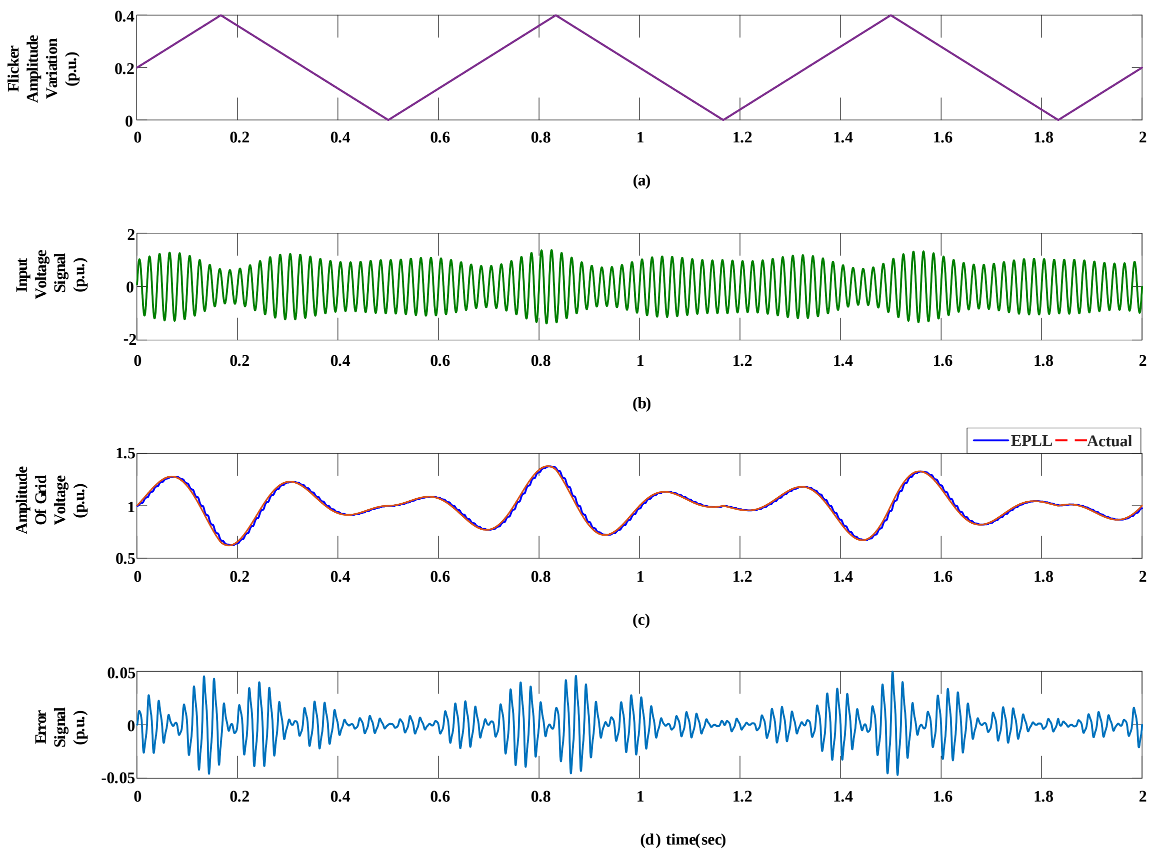

Figure 4.10: Estimation of amplitude of grid voltage for a flicker amplitude variation within 0-0.4 p.u. applying EPLL, where f_F = 5 Hz (a) Flicker Amplitude Variation(p.u.) (b) Input Voltage Signal(p.u.) (c) Amplitude of grid voltage(p.u.) (d) Error signal(p.u.).

4.3.10: Case-C3: Estimation of amplitude of grid voltage in case of variation of flicker amplitude and flicker frequency simultaneously

In this case both flicker amplitude and frequency is varied in a sinusoidal and triangular manner, respectively to reflect the practical scenario of flicker that neither its amplitude nor frequency is constant. From fig 4.11(d) it is observed that the system tracks more accurately when both the flicker amplitude and frequency is low or decreasing.

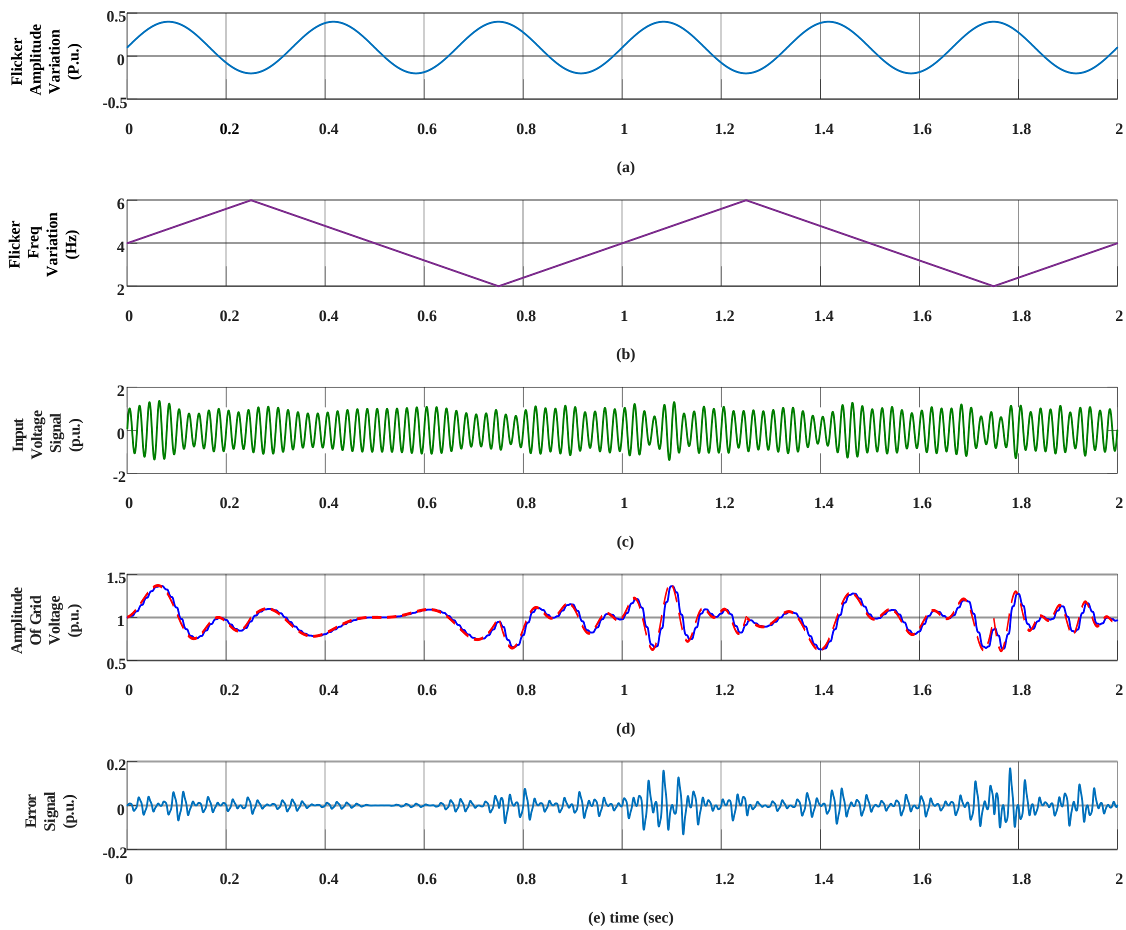

Figure 4.11: Estimation of amplitude of grid voltage for a variation of flicker amplitude and frequency simultaneously applying EPLL, where AF= -0.2-0.4 p.u. and f_F = 2-6 Hz (a) Flicker Amplitude Variation(p.u.) (b) Flicker Frequency Variation(Hz) (c) Input Voltage Signal(p.u.) (d) Amplitude of grid voltage(p.u.) (e) Error signal(p.u.).

4.4 Case-A: Estimation of Voltage flicker from time varying grid voltage applying EPLL and EKF simultaneously

4.4.1: Case-A1: Sinusoidal variation of instantaneous flicker

In this case the grid voltage of fundamental frequency 50 Hz is suffering from a sinusoidal flicker of amplitude 0.2 p.u. and frequency 5 Hz as shown in fig 4.12 (a). An enhanced PLL is applied to extract the envelope of this voltage which contains the fundamental amplitude plus flicker as shown in fig 4.12 (b). This envelope is applied as input to the EKF to estimate the instantaneous flicker level as shown in fig 4.12(c).

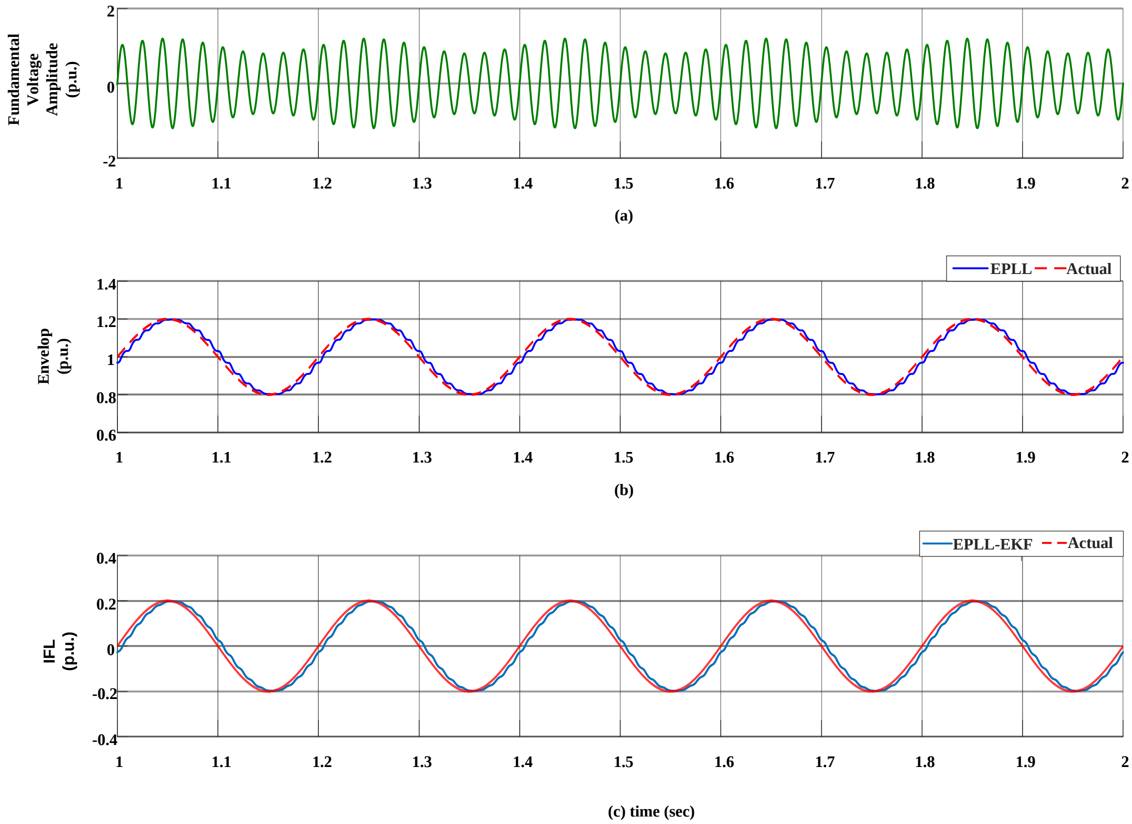

Figure 4.12: Estimation of sinusoidal variation of instantaneous flicker from time varying grid voltage applying EPLL and EKF simultaneously, where AF = 0.2 p.u. and f_F = 5 Hz (a) Fundamental voltage amplitude (b) Envelope extracted by EPLL (c) Instantaneous flicker level (IFL).

4.4.2: Case-A2: Triangular variation of instantaneous flicker

In this case the grid voltage of fundamental frequency 50 Hz is suffering from a triangular flicker of amplitude 0.2 p.u. and frequency 5 Hz as shown in fig 4.13 (a). An enhanced PLL is applied to extract the envelope of this voltage which contains the fundamental amplitude plus flicker as shown in fig 4.13 (b). This envelope is applied as input to the EKF to estimate the instantaneous flicker level as shown in fig 4.13(c).

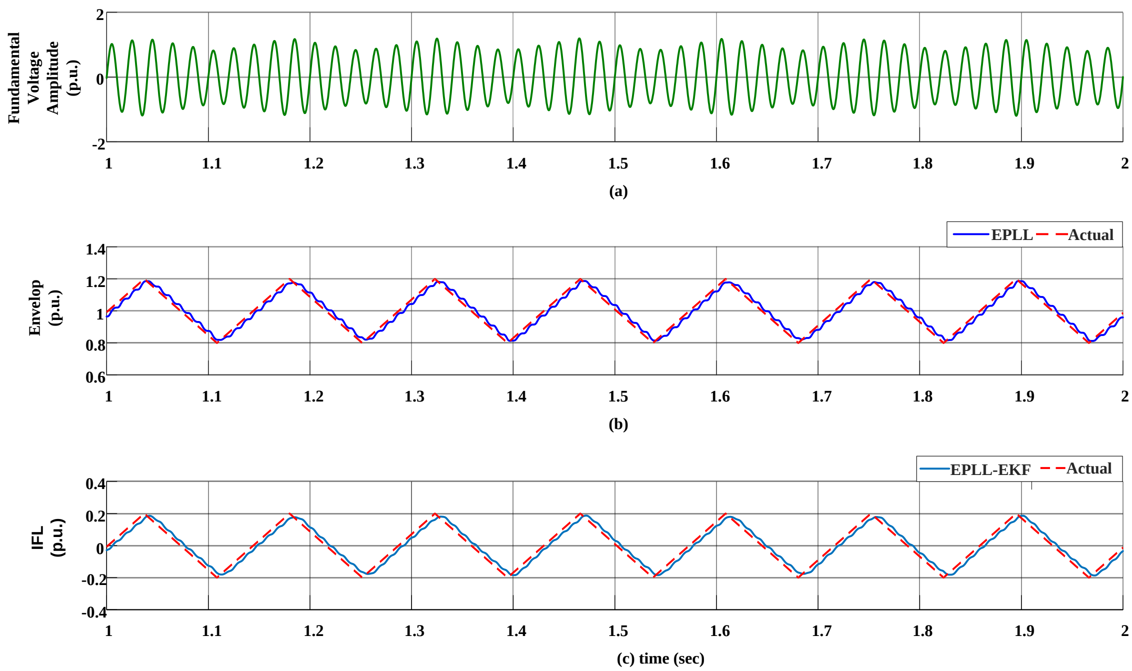

Figure 4.13: Estimation of triangular variation of instantaneous flicker from time varying grid voltage applying EPLL and EKF simultaneously, where AF = 0.2 p.u. and fF = 7 Hz (a) Fundamental voltage amplitude (b) Envelope extracted by EPLL (c) Instantaneous flicker level (IFL).

4.4.3: Case-A3: Square variation of instantaneous flicker

In this case the grid voltage of fundamental frequency 50 Hz is suffering from a square flicker of amplitude 0.2 p.u. and frequency 5 Hz as shown in fig 4.14 (a). An enhanced PLL is applied to extract the envelope of this voltage which contains the fundamental amplitude plus flicker as shown in fig 4.14 (b). This envelope is applied as input to the EKF to estimate the instantaneous flicker level as shown in fig 4.14(c).

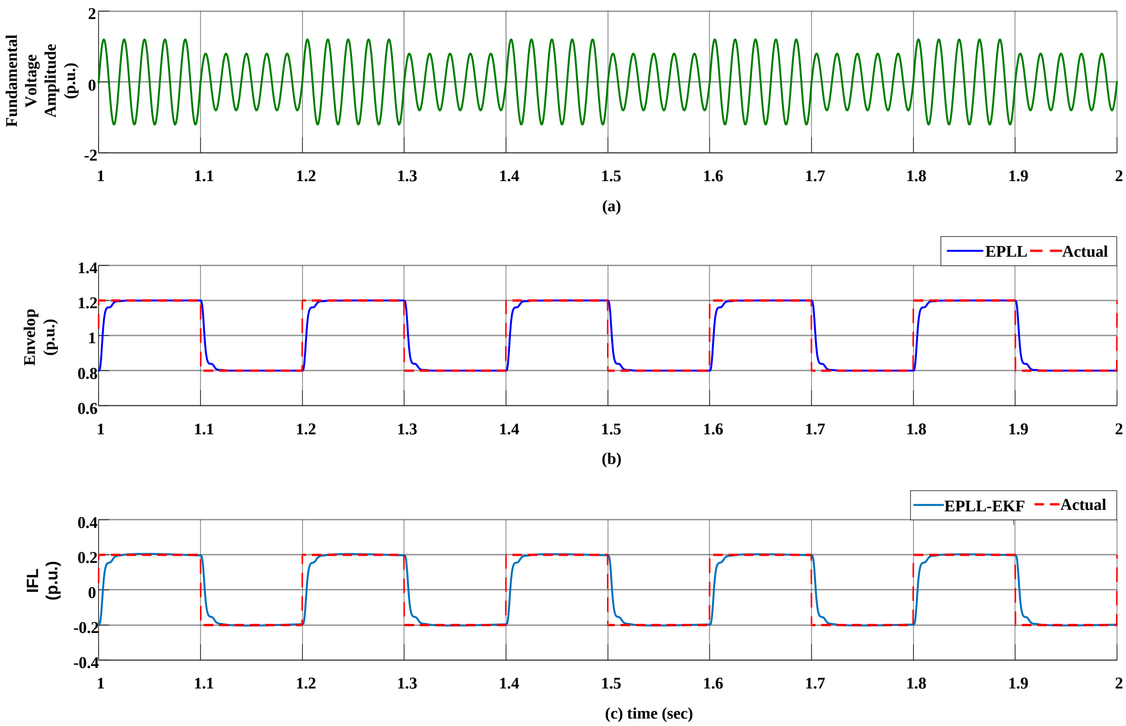

Figure 4.14: Estimation of square variation of instantaneous flicker from time varying grid voltage applying EPLL and EKF simultaneously, where AF = 0.2 p.u. and f_F = 5 Hz (a) Fundamental voltage amplitude (b) Envelope extracted by EPLL (c) Instantaneous flicker level (IFL).

4.4.4: Case-A4: Sawtooth variation of instantaneous flicker

In this case the grid voltage of fundamental frequency 50 Hz is suffering from a sawtooth flicker of amplitude 0.2 p.u. and frequency 5 Hz as shown in fig 4.15 (a). An enhanced PLL is applied to extract the envelope of this voltage which contains the fundamental amplitude plus flicker as shown in fig 4.15 (b). This envelope is applied as input to the EKF to estimate the instantaneous flicker level as shown in fig 4.15(c).

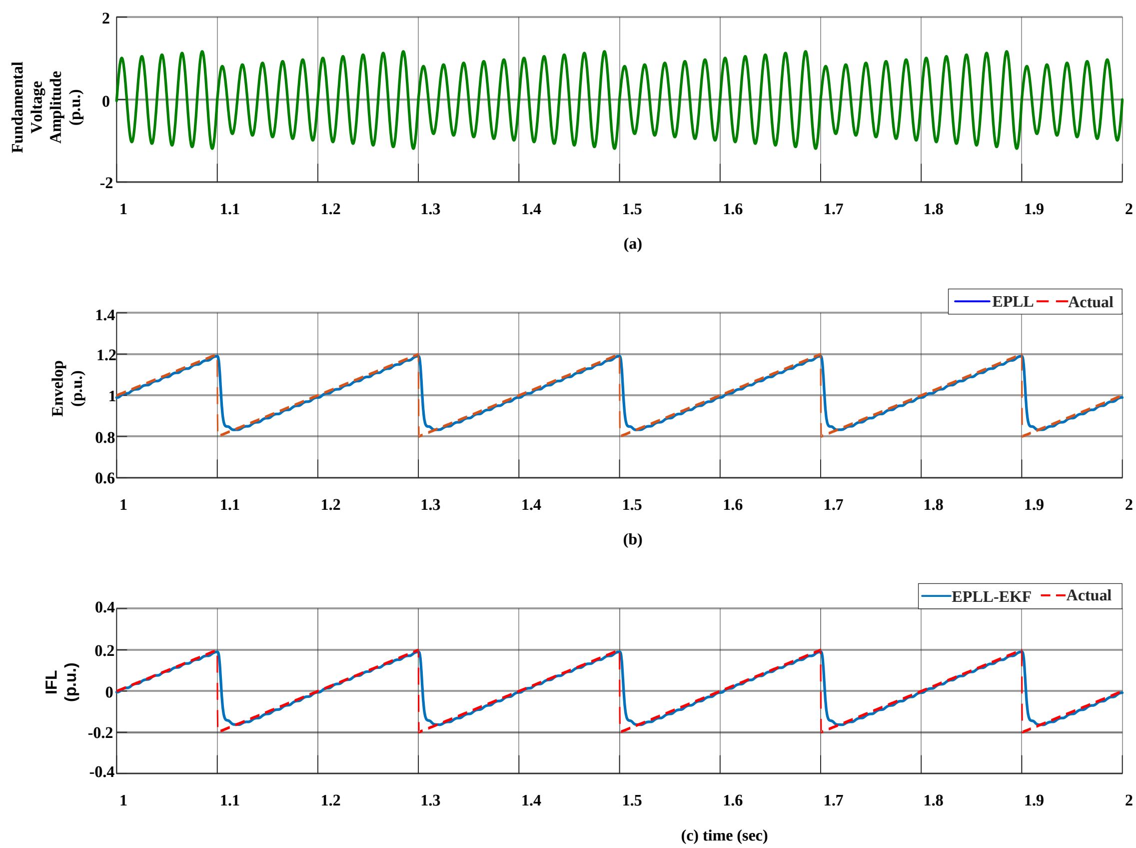

Figure 4.15: Estimation of sawtooth variation of instantaneous flicker from time varying grid voltage applying EPLL and EKF simultaneously, where AF = 0.2 p.u. and f_F = 5 Hz (a) Fundamental voltage amplitude (b) Envelope extracted by EPLL (c) Instantaneous flicker level (IFL).

4.4.5: Case-B1: Estimation of instantaneous flicker for a fundamental frequency rather than the nominal frequency

In this case a fundamental frequency (f) of 48 Hz is used instead of the nominal 50 Hz to test the performance of the proposed EPLL-EKF technique in a situation where grid voltage is subjected to any phase instability. The grid voltage also suffers from a sinusoidal flicker. The system starts tracking more accurately after a few msec.

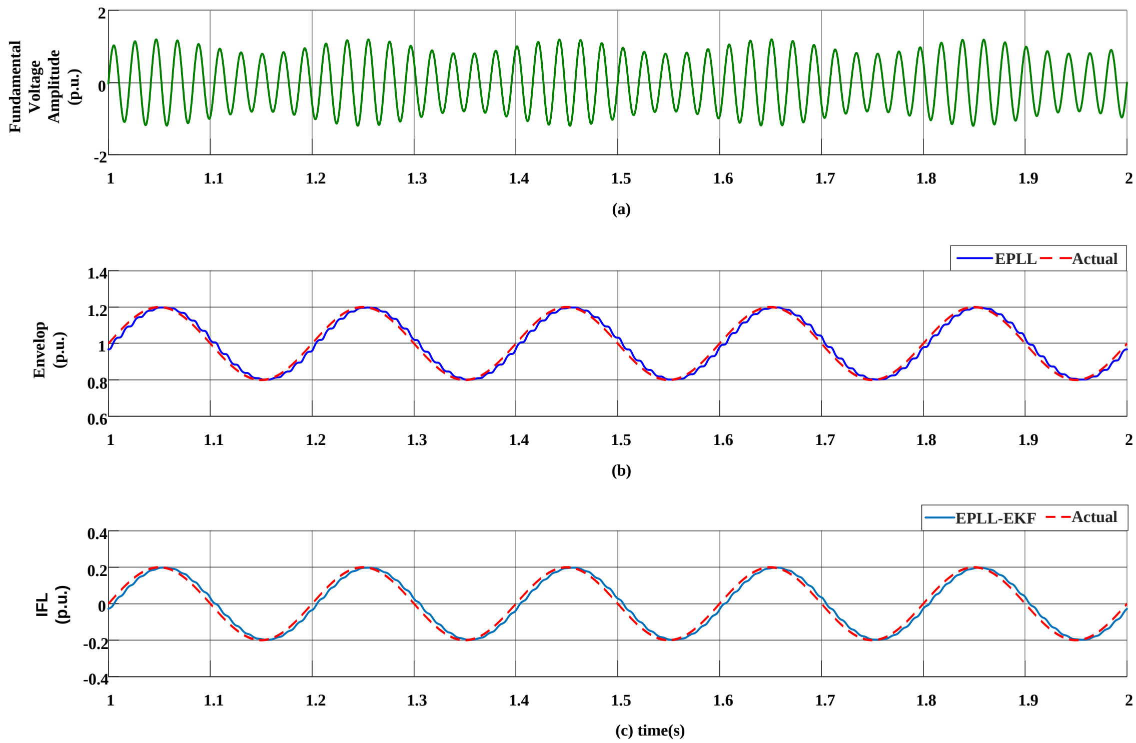

Figure 4.16: Estimation of instantaneous flicker for fundamental frequency 48 Hz applying EPLL and EKF simultaneously, where AF = 0.2 p.u. and fF = 5 Hz (a) Fundamental voltage amplitude (b) Envelope extracted by EPLL (c) Instantaneous flicker level (IFL).

4.4.6: Case-B2: Estimation of instantaneous flicker for a fundamental frequency rather than the nominal frequency

In this case a fundamental frequency (f) of 52 Hz is used instead of the nominal 50 Hz to test the performance of the proposed EPLL-EKF technique in a situation where grid voltage is subjected to any phase instability. The grid voltage also suffers from a sinusoidal flicker. The system starts tracking more accurately after a few msec.

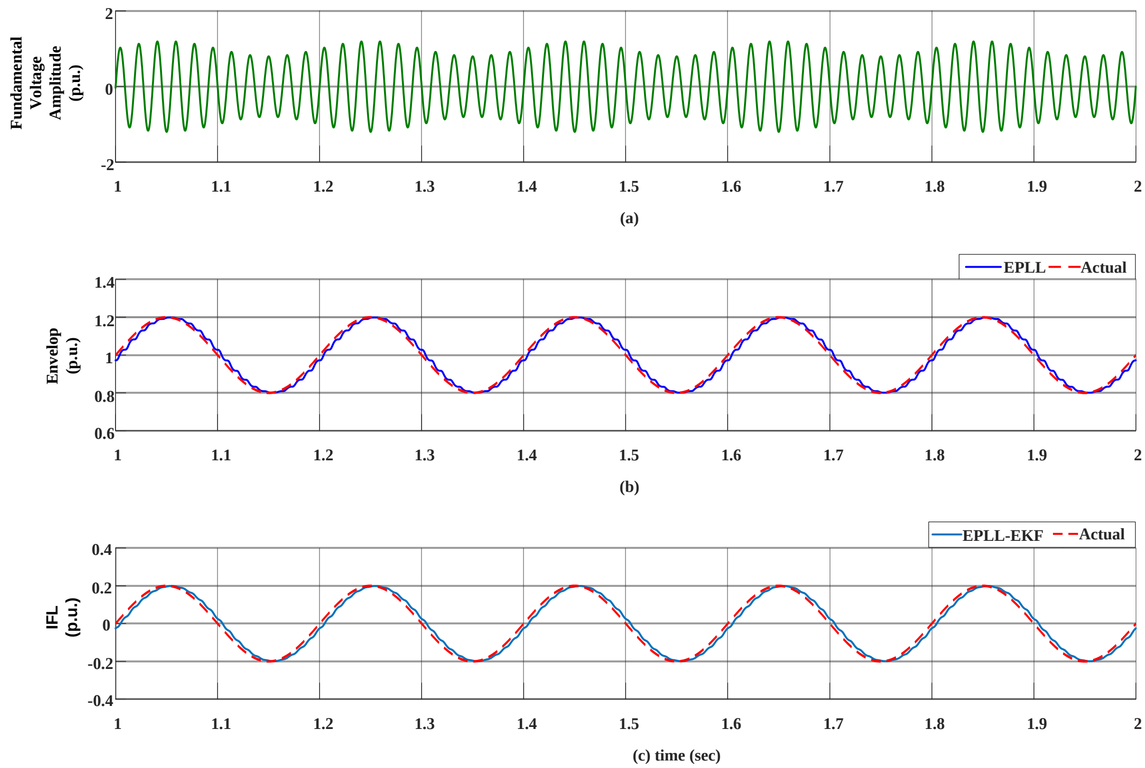

Figure 4.17: Estimation of instantaneous flicker for fundamental frequency 52 Hz applying EPLL and EKF simultaneously, where AF = 0.2 p.u. and fF = 5 Hz (a) Fundamental voltage amplitude (b) Envelope extracted by EPLL (c) Instantaneous flicker level (IFL).

4.4.7: Case-B3: Estimation of instantaneous flicker in case of a variation of fundamental frequency rather than the constant nominal frequency

In this case the fundamental frequency is considered to be changing periodically rather than a constant value. It is varied linearly within 45 to 55 Hz in order to demonstrate the time varying frequency tracking capability of the proposed EPLL-EKF technique. It is observed that the system starts tracking more accurately after a few msec.

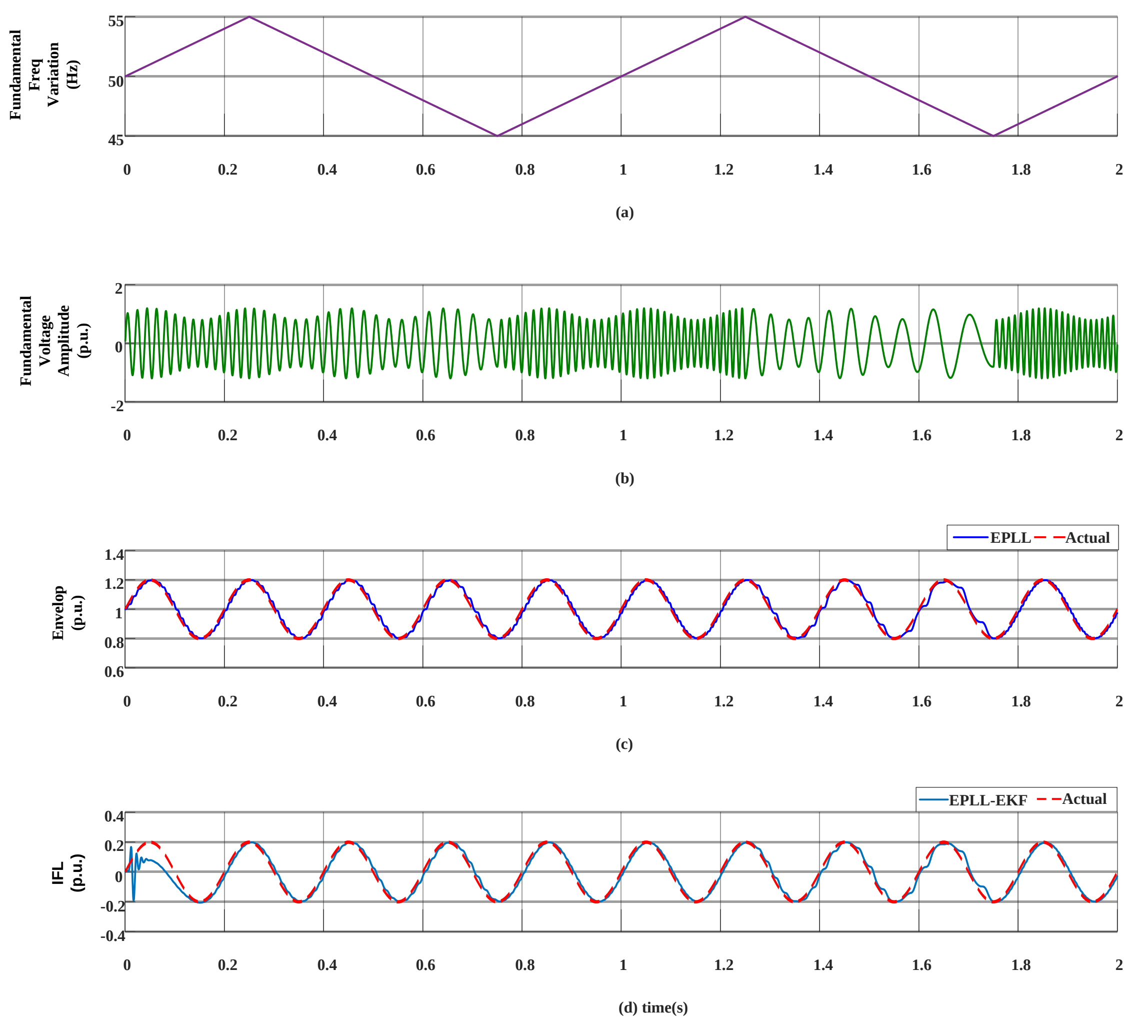

Figure 4.18: Estimation of instantaneous flicker for a fundamental frequency variation within 45-55 Hz applying EPLL and EKF simultaneously, where AF = 0.2 p.u. and f_F = 5 Hz (a) fundamental frequency variation(Hz) (b) Fundamental voltage amplitude (c) Envelope extracted by EPLL (d) Instantaneous flicker level (IFL).

4.4.8: Case-C1: Estimation of instantaneous flicker in case of a variation of flicker frequency only

In this case the flicker frequency is varied from 2 Hz to 6 Hz in a triangular manner to reflect the practical scenario of flicker that its frequency is not constant. From fig 4.19(d) it is observed that the system better tracks the flicker after a few ms of simulation.

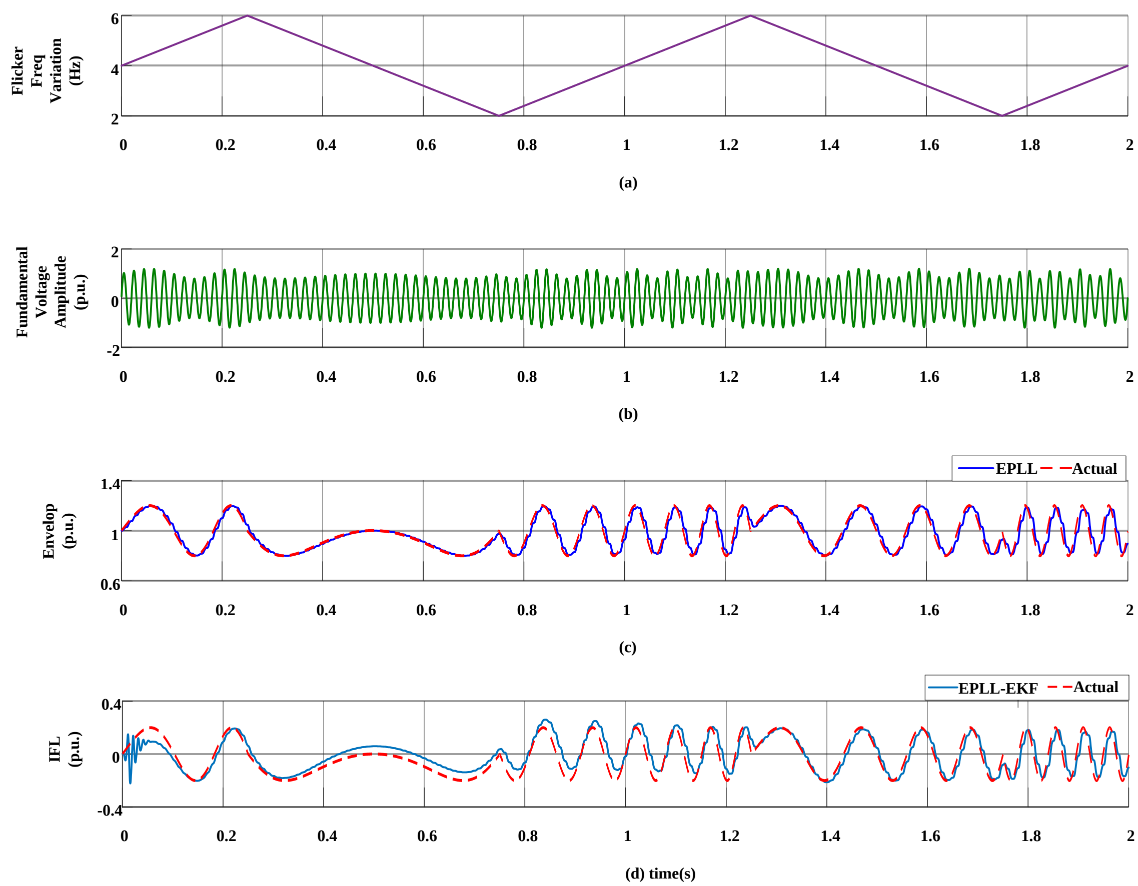

Figure 4.19: Estimation of instantaneous flicker for a flicker frequency variation within 2-6 Hz applying EPLL and EKF simultaneously, where AF = 0.2 p.u. (a) Flicker frequency variation(Hz) (b) Fundamental voltage amplitude (c) Envelope extracted by EPLL (d) Instantaneous flicker level (IFL).

4.4.9: Case-C2: Estimation of instantaneous flicker in case of a variation of flicker amplitude only

In this case the flicker amplitude is varied from 0 to 0.4 p.u. in a triangular manner to reflect the practical scenario of flicker that its amplitude is not constant. From fig 4.20(d) it is observed that the system better tracks the flicker after a few milliseconds of simulation.

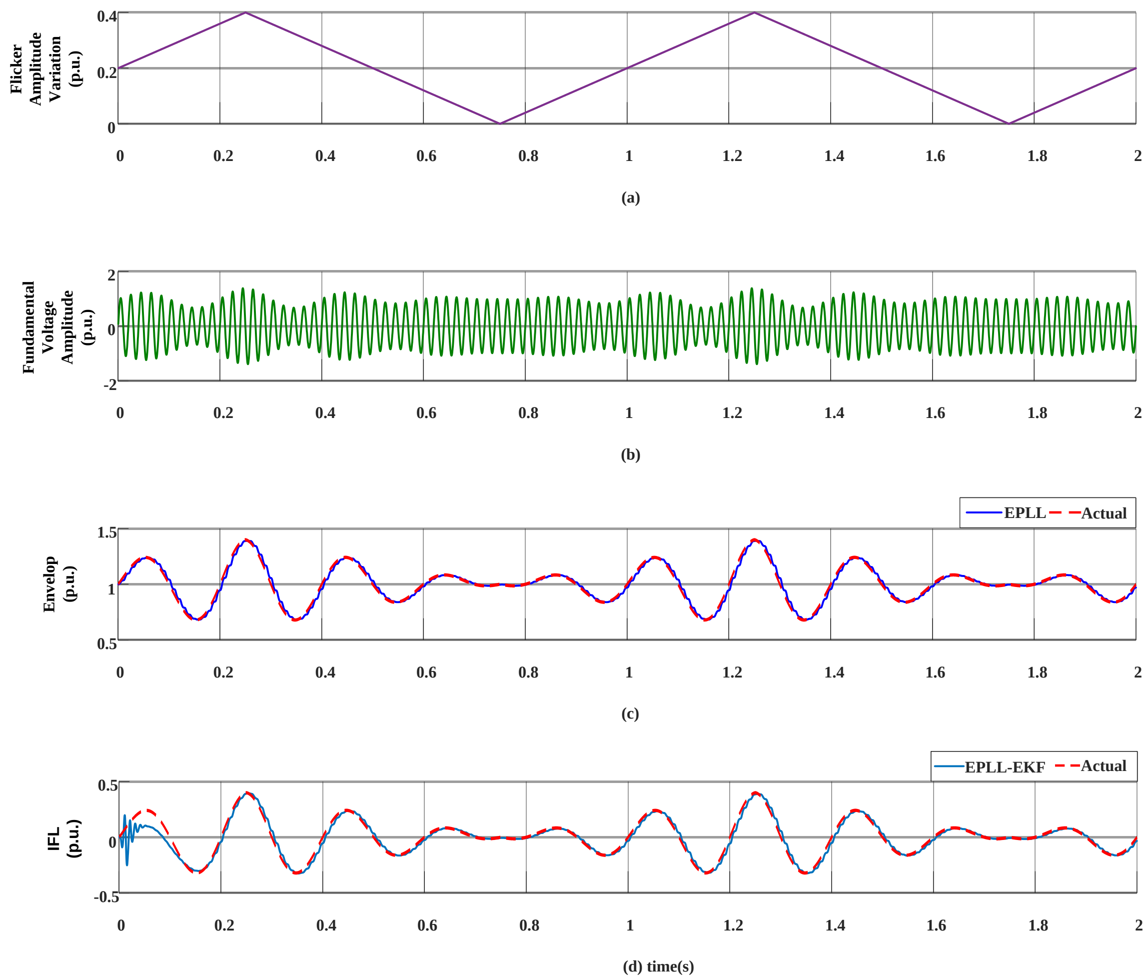

Figure 4.20: Estimation of instantaneous flicker for a flicker amplitude variation within 0-0.4 p.u. applying EPLL and EKF simultaneously, where f_F = 5 Hz (a) Flicker Amplitude variation(p.u.) (b) Fundamental voltage amplitude (c) Envelope extracted by EPLL (d) Instantaneous flicker level (IFL).

4.4.10: Case-C3: Estimation of instantaneous flicker in case of variation of flicker amplitude and flicker frequency simultaneously

In this case both flicker amplitude and frequency is varied in a triangular manner to reflect the practical scenario of flicker that neither its amplitude nor frequency is constant. From fig 4.21(d) it is observed that the system tracks more accurately after a few ms of simulation.

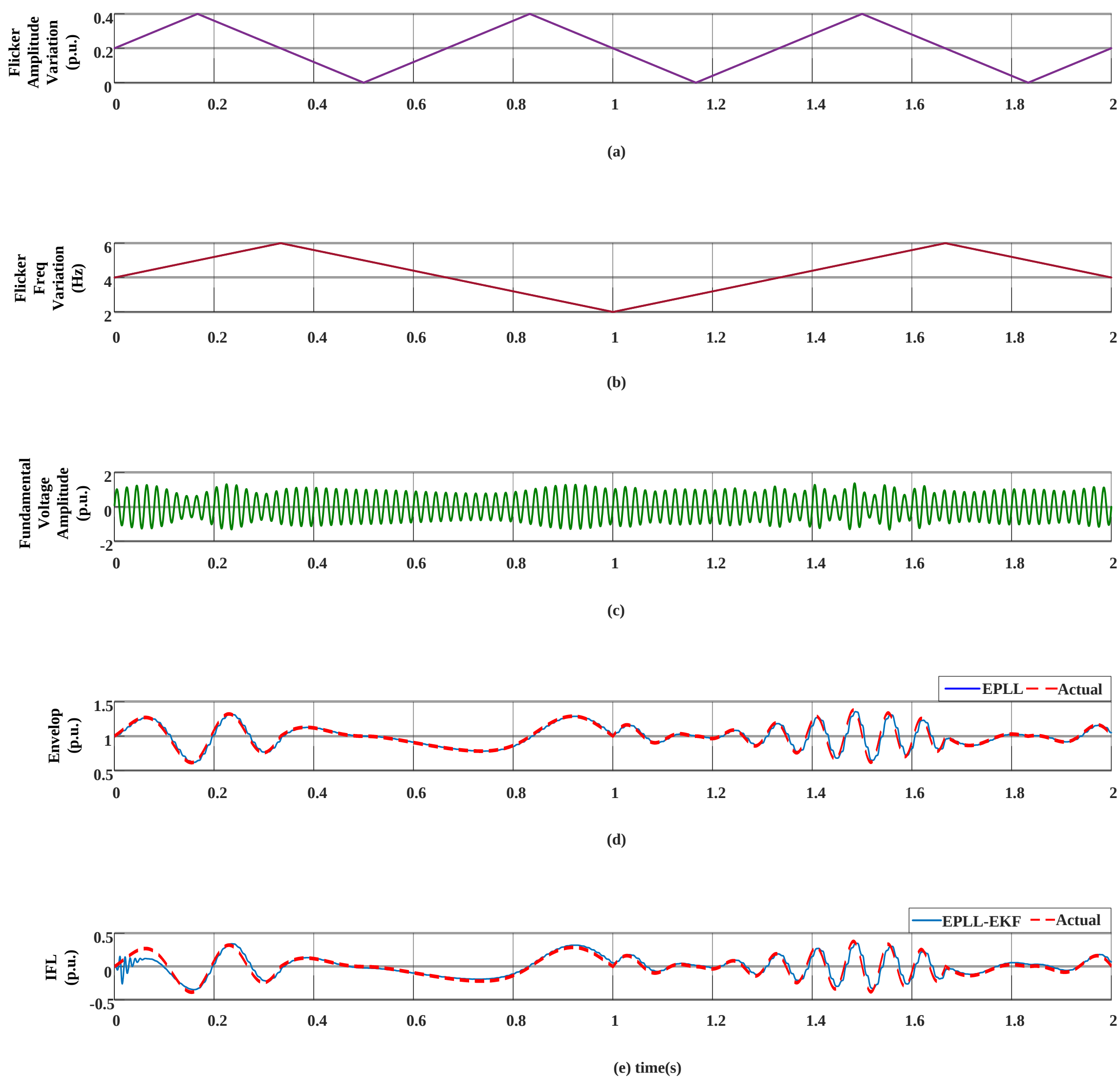

Figure 4.21: Estimation of instantaneous flicker for variation of flicker amplitude and frequency simultaneously applying EPLL and EKF simultaneously, where AF=0-0.4 p.u. and f_F = 2-6 Hz (a) Flicker Amplitude variation (p.u.) (b) Flicker frequency variation(Hz)

(c) Fundamental voltage amplitude (d) Envelope extracted by EPLL (e) Instantaneous flicker level (IFL).

Chapter 5: Conclusions

This chapter summarizes the objectives and the methodologies combined in one section that is the Summary in 5.1. The section 5.2 indicates the future aspects and how the techniques can be further developed.

5.1 Summary

In this thesis work we developed a Kalman filtering technique that is capable of accurately estimating flicker in the grid system. The system also has an Enhanced Phase Locked Loop (EPLL) coupled to the filter. The combination of the filter and the EPLL can successfully track different types of flicker with different frequencies and combinations of both. But the system doesn't take into account harmonics. Harmonics is present in the grid but we have not taken it into account for ease of calculation. This is the drawback of the developed Kalman filter. The filter and EPLL were both developed using MATLAB.

The developed Kalman filter can endure frequency changes in both the grid and flicker voltage. It is very efficient at tracking flicker through the algorithm that has been developed. The whole system is non-linear. The purpose of this system is to quickly predict and track voltage drops due to cyclic and non-cyclic flicker so that instruments that rely on constant power can take action to protect it from damage due to flicker. This can greatly improve the life time of electrical appliances and industrial machines. The system needs further development to put it into implementation phase.

5.2 Future Work

The purpose of the thesis work was to estimate flicker using Kalman filter in a fast and accurate way. Types of Kalman filter and EPLL has been discussed. The code generated for the purpose of this thesis is such that it can handle different types of flicker. We used Kalman filter to estimate flicker in a grid system and also used different combinations and types of flicker to determine and record the results. But we did not take in account the harmonics that are present in the grid system. We would like to further extend this research by taking into account the harmonics and other problems that come with it. The code that we have produced to track and estimate flicker can also be made more efficient with time and effort. After that we will try to implement this system on the grid to check its reliability.

The current filter that has been designed can track and estimate flicker but it can be improved to make it more accurate and fast. Furthermore, harmonics was not taken into account but if we add harmonics detection the designed filter will be able to track and estimate flicker even if there are the above mentioned problems. The complete system can then be implemented in the grid system to check its reliability and accuracy in real time. This might help with the compensation of the voltage drops due to flicker and further improve the life of household and other electrical appliances. As the Kalman technique used in this thesis paper is complex we want to introduce a simpler and more efficient technique that might be easily applicable in the real world.

1. Spring, A., et al, "Effects of Flicker in a Distribution Grid with high PV Penetration.", 28th European Photovoltaic Solar Energy Conference and Exhibition. 2013.

2. Dugan, R.C., M.F. McGranaghan, and H.W. Beaty, "Electrical power systems quality." New York, NY: McGraw-Hill,| c1996, 1996.

3. Yan, T., et al., "The Research of Voltage Flicker Detection Based on IRPT and Mitigation Based on BESS.", International Conference on Computer Information Systems and Industrial Applications, Atlantis Press.2015.

4. Renner, H, "Flicker source identification in meshed high voltage grids.", Electric Power Quality and Supply Reliability Conference (PQ), 2012. IEEE press, 2012.

5. Gutierrez, J., et al., "Measurement of Voltage Flicker: Application to Grid-connected Wind Turbines, in Advances in Measurement Systems.", InTech. 2010,

6. Liu, X., et al, "Investigation of the transmission line impedance effects on voltage quality and flicker emission for grid connected to wind turbines.", Power Electronics and Motion Control Conference, 2009. IPEMC'09. IEEE 6th International. 2009. IEEE.

7. Sun, T., Z. Chen, and F. Blaabjerg, "Flicker study on variable speed wind turbines with doubly fed induction generators." *IEEE Transactions on Energy Conversion*, 2005. **20**(4): p. 896-905.

8. Papadopoulos, M., et al, "Voltage quality change by grid-connected wind turbines.", EWEC-CONFERENCE-. 1999.

9. Amaris, H., J. Usaola, and C. Vilar, "A more realistic flicker coefficient for wind turbines evaluation.", EWEC-CONFERENCE-. 1999.

10. Papadopoulos, M., et al., "Investigation of the flicker emission by grid connected wind turbines.", *Harmonics and Quality of Power Proceedings*, 1998. Proceedings. 8th International Conference On. 1998. IEEE.

11. Alkandari, A. and S. Soliman, "Measurement of a power system nominal voltage, frequency and voltage flicker parameters." *International Journal of Electrical Power & Energy Systems, 2009.* **31**(7): p. 295-301.

12. Cavallini, A., et al., "Atp simulation for arc-furnace flicker investigation." *International Transactions on Electrical Energy Systems, 1995*. **5**(3): p. 165-172.

13. Natarajan, R., et al., "Determination of Flicker Effects Due to An Electric Arc Furnace. in Proceedings of the American Power Conference.", ILLINOIS INSTITUTE OF TECHNOLOGY. 1994.

14. Simoes, M.C. and S. Deckmann, "Flicker propagation and attenuation.", *Harmonics and Quality of Power, 2002.* 10th International Conference on. 2002. IEEE.

15. Commission, I.E., "Flickermeter-Functional and design specifications." *IEC Report*. Publication, 1986. **868**.

16. Renner, H. and M. Sakulin, "Flicker propagation in meshed high voltage networks.", *Harmonics and Quality of Power, 2000,* Ninth International Conference on. 2000. IEEE.

17. Zhang, D., W. Xu, and A. Nassif. "Flicker source identification by interharmonic power direction.", *Electrical and Computer Engineering, 2005,* Canadian Conference on. 2005. IEEE.

18. Walker, M.K., "Electric utility flicker limitations.", *IEEE Transactions on Industry applications*, 1979(6): p. 644-655.

19. Saad-Saoud, Z. and N. Jenkins, "Models for predicting flicker induced by large wind turbines.", *IEEE Transactions on Energy Conversion*, 1999. **14**(3): p. 743-748.

20. Majchrzak, J. and G. Wiczyński, "Basic characteristics of IEC flickermeter processing.", *Modelling and Simulation in Engineering, 2012*. **2012**: p. 42.

21. law Majchrzak, J. and G. Wiczynski, "Basic characteristics of IEC flickermeter processing.", *Hindawi Publishing Corporation Modelling and Simulation in Engineering Volume 2012,* Article ID 362849, 30 November 2012

22. Al-Hamadi, H., "Fuzzy logic voltage flicker estimation using Kalman filter." *International Journal of Electrical Power & Energy Systems, 2012*. **36**(1): p. 60-67.

23. Al-Hamadi, H., "Fuzzy Logic Voltage Flicker Estimation Using Hilbert Transform.", International Conference on Mechanical Engineering and Technology (ICMET-London 2011). 2011. ASME Press.

24. Al-Hamadi, H. and S. Soliman. "Estimating Instantaneous Voltage Flicker Using Kalman Filter And Fuzzy Logic tuning Noise Levels.", Proceedings of IASTED International Conference on Power and Energy Systems (EuroPES 2007) in Palma de Mallorca, Spain. 2007.

25. Ashmole, P. and P. Amante, "System flicker disturbances from industrial loads and their compensation.", *Power Engineering Journal, 1997*. **11**(5): p. 213-218.

26. Power quality basics: voltage fluctuations and flicker- http://www.powerqualityworld.com/2011/09/voltage-fluctuations-flicker.html

27. Baggini, A., "Handbook of power quality.", 2008.

28. Luo, X., et al., "Overview of current development in electrical energy storage technologies and the application potential in power system operation.", *Applied Energy, 2015*. **137**: p. 511-536.

29. Arrillaga, J., Y.H. Liu, and N.R. Watson, "Flexible power transmission: the HVDC options.", 2007.

30. Group, I.P.W., "Recommended practice for monitoring electric power quality.", Technical report, Draft 5. 1994.

31. Agüero, J.R. "Improving the efficiency of power distribution systems through technical and non-technical losses reduction.", Transmission and Distribution Conference and Exposition (T&D), 2012, *IEEE PES*. 2012. IEEE.

32. Mendis, S., M. Bishop, and J. Witte. "Investigations of voltage flicker in electric arc furnace power systems.", *Industry Applications Society Annual Meeting, 1994.*, Conference Record of the 1994 IEEE. 1994. IEEE.

33. Elnady, A. and M.M. Salama, "Unified approach for mitigating voltage sag and voltage flicker using the DSTATCOM." *IEEE transactions on power delivery, 2005.* **20**(2): p. 992-1000.

34. Montanari, G., et al., "Arc-furnace model for the study of flicker compensation in electrical networks." *IEEE Transactions on Power Delivery, 1994.* **9**(4): p. 2026-2036.

35. Girgis, A.A. and E.B. Makram. "Measurement of voltage flicker magnitude and frequency using a Kalman filtering based approach.", *Electrical and Computer Engineering, 1996.* Canadian Conference on. 1996. IEEE.

36. Nassif, A., E.E. Nino, and W. Xu. "A VI slope-based method for flicker source detection. in Power Symposium, 2005." *Proceedings of the 37th Annual North American*. 2005. IEEE.

37. Mendis, S., et al., "Investigation of transmission system voltage flicker due to multiple ac and dc furnace operations." *IEEE transactions on power delivery, 1995.* **10**(1): p. 483-496.

38. Fallen, C. and B.A. McDermott. "Development and testing of a real-time digital voltage flickermeter.", *Transmission and Distribution Conference, 1996. Proceedings., 1996 IEEE*. 1996. IEEE.

39. Zheng, T. and E.B. Makram, "Wavelet representation of voltage flicker." *Electric Power Systems Research*, 1998. **48**(2): p. 133-140.

40. FLicker in the power master series- http://www.rangerpq.com/flicker.html

41. Wang, C.-S. and M.J. Devaney, "Incandescent lamp flicker mitigation and measurement." *IEEE Transactions on Instrumentation and measurement,* 2004. **53**(4): p. 1028-1034.

42. Keppler, T., N. Watson, and J. Arrillaga, "Computation of the short-term flicker severity index." *IEEE Transactions on power delivery,* 2000. **15**(4): p. 1110-1115.

43. Caldara, S., S. Nuccio, and C. Spataro, "A virtual instrument for measurement of flicker." *IEEE Transactions on instrumentation and measurement,* 1998. **47**(5): p. 1155-1158.

44. Newman Jr, R.C., D.F. Hausman, and R.C. Moseley, "Phase controlled dimming system with active filter for preventing flickering and undesired intensity changes.", Google Patents, 2000,

45. Bullough, J.D., et al., "Detection and acceptability of stroboscopic effects from flicker." *Lighting Research & Technology,* 2012. **44**(4): p. 477-483.

46. Effects of voltage fluctuations on electrical and electronic equipment http://www.powerqualityworld.com/2011/09/effects-voltage-fluctuations.html

47. Hanzelka, Z. and A. Bien, "Voltage disturbances. Flicker measurement." *Power Quality Application Guide, copper development association*, 2005: p. 1-12.

48. Finley, W.R., M. Howdowanec, and W.G. Holter. "Diagnosing motor vibration problems.", Pulp and Paper Industry Technical Conference, 2000. Conference Record of 2000 Annual. 2000. IEEE.

49. Maglinao Jr, A.L., "Development of a segregated municipal solid waste gasification system for electrical power generation.", Texas A&M University, 2013.

50. Hall, P.J. and E.J. Bain, "Energy-storage technologies and electricity generation." *Energy policy, 2008.* **36**(12): p. 4352-4355.

51. Ibrahim, H., A. Ilinca, and J. Perron, "Energy storage systems—characteristics and comparisons." *Renewable and sustainable energy reviews,* 2008. **12**(5): p. 1221-1250.

52. Marei, M., E. El-Saadany, and M. Salama, "Estimation techniques for voltage flicker envelope tracking.", *Electric Power Systems Research*, 2004. **70**(1): p. 30-37.

53. Sachdev, M. and M. Nagpal, "A recursive least error squares algorithm for power system relaying and measurement applications." *IEEE Transactions on Power Delivery*, 1991. **6**(3): p. 1008-1015.

54. Chen, M., "Digital algorithms for measurement of voltage flicker.", *IEE Proceedings-Generation, Transmission and Distribution,* 1997. **144**(2): p. 175-180.

55. Sadinezhad, I. and V.G. Agelidis, "Frequency adaptive least-squares-Kalman technique for real-time voltage envelope and flicker estimation.", *IEEE Transactions on Industrial Electronics,* 2012. **59**(8): p. 3330-3341.

56. Chang, G.W., et al., "On real-time simulation for harmonic and flicker assessment of an industrial system with bulk nonlinear loads.", *IEEE Transactions on Industrial Electronics,* 2010. **57**(9): p. 2998-3009.

57. Axelberg, P.G., M.H. Bollen, and I.Y.-H. Gu, "Trace of flicker sources by using the quantity of flicker power." *IEEE transactions on Power Delivery,* 2008. **23**(1): p. 465-471.

58. Elnady, A. and M.M. Salama, "Unified approach for mitigating voltage sag and voltage flicker using the DSTATCOM.", *IEEE transactions on power delivery*, 2005. **20**(2): p. 992-1000.

59. Girgis, A.A., J.W. Stephens, and E.B. Makram, "Measurement and prediction of voltage flicker magnitude and frequency.", *IEEE Transactions on Power Delivery*, 1995. **10**(3): p. 1600-1605.

60. Chang, G.W., C.-I. Chen, and Y.-L. Huang, "A digital implementation of flickermeter in the hybrid time and frequency domains.", *IEEE Transactions on Power Delivery,* 2009. **24**(3): p. 1475-1482.

61. Kamwa, I. and R. Grondin, "Fast adaptive schemes for tracking voltage phasor and local frequency in power transmission and distribution systems.", *IEEE Transactions on Power Delivery,* 1992. **7**(2): p. 789-795.

62. Bettayeb, M. and U. Qidwai, "Recursive estimation of power system harmonics.", *Electric power systems research*, 1998. **47**(2): p. 143-152.

63. Johansson, R., "System modeling and identification.", Prentice-hall, 1993.

64. Ljung, L., "Theory for the User." Prentice Hall, 1987.

65. Langella, R. and A. Testa, " Electromagnetic compatibility (EMC)—Testing and measurement techniques—Flickermeter—Functional and design specifications. 2011.", *IEEE Recommended Practice—Adoption of IEC 61000-4-15: 2010,* 2011.

66. Albistur, C.F., et al., "A simple predictive method to estimate flicker.", *IEEE Transactions on Industry Applications*, 2014. **50**(3): p. 2150-2155.

67. Jin, H. and Y. Hong-geng, "An Approach for Harmonic/Inter-harmonic Analysis Based on the Odd Points Interpolation Correction [J].", *Proceedings of the CSEE,* 2010. **30**(16): p. 67-72.

68. Li, F. and M. Ye. "Calculation of Flicker Parameters Using Voltage Interharmonics.", *Power and Energy Engineering Conference (APPEEC), 2012* Asia-Pacific. 2012. IEEE.

69. Gallo, D., et al. "IEC flickermeter response to interharmonic pollution.", *Harmonics and Quality of Power, 2004.* 11th International Conference on. 2004. IEEE.

70. Lemofouet, S. and A. Rufer, "Hybrid energy storage system based on compressed air and super-capacitors with maximum efficiency point tracking (MEPT)." *IEEJ Transactions on Industry Applications,* 2006. **126**(7): p. 911-920.

71. Genta, G., "Kinetic energy storage: theory and practice of advanced flywheel systems.", Butterworth-Heinemann, 2014.

72. Niu, G., "Electric-Hydraulic Hybrid Energy Storage System for Electrified Transportation.", Illinois Institute of Technology. 2017.

73. S E Haque, N H Malik, W'Shepherd, Sen, "Operation of a fixed capacitor-thyristor controlled reactor (FC-TCR) power factor compensator.", IEEE Transactions on Power Apparatus and Systems, Vol. PAS-104, No. 6, June 1985.

74. Bishop, G. and G. Welch, "An introduction to the Kalman filter.", *Proc of SIGGRAPH,* 2001. **8**(27599-23175): p. 41

75. Giroux, P., G. Sybille, and H. Le-Huy. "Modeling and simulation of a distribution STATCOM using simulink's power system blockset.", *Industrial Electronics Society, 2001. IECON'01.* The 27th Annual Conference of the IEEE. 2001. IEEE.

76. Farokhnia, N., et al. "Unbalance, flicker, harmonic, voltage and reactive power compensation of the distribution grid using a universal STATOM.", *Industrial Electronics (ISIE),* 2014 IEEE 23rd International Symposium on. 2014. IEEE.

77. Sun, J., D. Czarkowski, and Z. Zabar, "Voltage flicker mitigation using PWM-based distribution STATCOM.", *Power Engineering Society Summer Meeting, 2002 IEEE*. 2002. IEEE.

78. Sirisukprasert, S., "The modeling and control of a cascaded-multilevel converter-based STATCOM." 2004.

79. Ackermann, T., G. Andersson, and L. Söder, "Distributed generation: a definition.", *Electric power systems research,* 2001. **57**(3): p. 195-204.

80. Pepermans, G., et al., "Distributed generation: definition, benefits and issues.", *Energy policy,* 2005. **33**(6): p. 787-798.

81. Barker, P.P. and R.W. De Mello, "Determining the impact of distributed generation on power systems." *I. Radial distribution systems*. *IEEE*. 2000. IEEE.

82. Wang, C. and M.H. Nehrir, "Analytical approaches for optimal placement of distributed generation sources in power systems.", *IEEE Transactions on Power systems,* 2004. **19**(4): p. 2068-2076.

83. El-Khattam, W. and M.M. Salama, "Distributed generation technologies, definitions and benefits.", *Electric power systems research,* 2004. **71**(2): p. 119-128.

84. Fujita, H. and H. Akagi, "The unified power quality conditioner: the integration of series-and shunt-active filters.", *IEEE transactions on power electronics,* 1998. **13**(2): p. 315-322.

85. Akagi, H., "Trends in active power line conditioners.", *IEEE transactions on power electronics,* 1994. **9**(3): p. 263-268.

86. Grady, W.M., M.J. Samotyj, and A.H. Noyola, "Survey of active power line conditioning methodologies.", *IEEE Transactions on Power Delivery,* 1990. **5**(3): p. 1536-1542.

87. Van Wyk, J. "Power quality, power electronics and control.", *Power Electronics and Applications, 1993.,* Fifth European Conference on. 1993. IET.

88. Akagi, H., "New trends in active filters for power conditioning.", *IEEE transactions on industry applications,* 1996. **32**(6): p. 1312-1322.

89. Aredes, M., J. Hafner, and K. Heumann, "Three-phase four-wire shunt active filter control strategies." *IEEE Transactions on Power Electronics,* 1997. **12**(2): p. 311-318.

90. Cavallini, A. and G.C. Montanari, "Compensation strategies for shunt active-filter control." *IEEE Transactions on Power Electronics,* 1994. **9**(6): p. 587-593.

91. Jou, H.-L., "Performance comparison of the three-phase active-power-filter algorithms.", *IEE Proceedings-generation, transmission and distribution,* 1995. **142**(6): p. 646-652.

92. El-Habrouk, M., M. Darwish, and P. Mehta, "Active power filters: A review.", *IEE Proceedings-Electric Power Applications*, 2000. **147**(5): p. 403-413.

93. Fujita, H., H. Akagi, and M. Kohata, "Combined rectifying system including double-series capacitor-smoothed diode rectifier and series active filter.", *Electrical engineering in Japan*, 1997. **120**(1): p. 85-94.

94. Nastran, J., et al., "Active power filter for nonlinear AC loads.", *IEEE Transactions on Power Electronics*, 1994. **9**(1): p. 92-96.

95. Bhavaraju, V. and P. Enjeti, "A fast active power filter to correct line voltage sags.", *IEEE Transactions on Industrial Electronics*, 1994. **41**(3): p. 333-338.

96. Cho, G.C., et al., "Analysis and controller design of static var compensator using three-level GTO inverter.", *IEEE Transactions on Power Electronics,* 1996. **11**(1): p. 57-65.

97. Libano, F.B., D. Simonetti, and J. Uceda, "Frequency characteristics of hybrid filter systems.", *Power Electronics Specialists Conference, 1996. PESC'96 Record.,* 27th Annual IEEE. 1996. IEEE.

98. Manon, G., et al. "Design of a unified power flow controller for implementation into a micronetwork.", *European conference on power electronics and applications*. 1997.

99. Asao, T., et al. "Evaluation method of power rating and energy capacity of superconducting magnetic energy storage system for output smoothing control of wind farm.", *Electrical Machines, 2008. ICEM 2008.* 18th International Conference on. 2008. IEEE.

100. Buckles, W. and W.V. Hassenzahl, "Superconducting magnetic energy storage.", *IEEE Power Engineering Review*, 2000. **20**(5): p. 16-20.

101. Hassenzahl, W., "Superconducting magnetic energy storage.", *IEEE Transactions on magnetics,* 1989. **25**(2): p. 750-758.

102. Campbell, A., "Superconducting Magnetic Energy Storage (SMES).", *Renewable Energy Storage*: p. 45-50.

103. Kamwa, I. and K. Srinivasan, "A Kalman filter-based technique for combined digital estimation of voltage flicker and phasor in power distribution systems.", *International Transactions on Electrical Energy Systems*, 1993. **3**(2): p. 131-142.

104. Jacobs93 Jacobs, O. L. R. "Introduction to Control Theory, 2nd Edition.", 1993.

105. BROWN, R. and P. HWANG, "Introduction to random signals and applied Kalman filtering(Book).", 1992. 512, 1992.

106. Gelb, A., "Applied optimal estimation.", MIT press, 1974.

107. Lewis86 Lewis, Richard. "Optimal Estimation with an Introduction to Stochastic Control Theory.", John Wiley & Sons, Inc, 1986.

108. Maybeck, Peter S, "Stochastic Models, Estimation, and Control, Volume1." Academic Press, Inc, 1979.

109. Julier, S.J. and J.K. Uhlmann, "A general method for approximating nonlinear transformations of probability distributions.", Robotics Research Group, Department of Engineering Science, University of Oxford, Oxford, OC1 3PJ United Kingdom, Tech. Rep, 1996.

110. Karimi-Ghartemani, M. and M. Iravani. "A new phase-locked loop (PLL) system.", *Circuits and Systems, 2001. MWSCAS 2001.* 44th IEEE 2001 Midwest Symposium on. 2001. IEEE.

111. Karimi-Ghartemani, M., "Enhanced Phase-Locked Loop.", *Enhanced Phase-Locked Loop Structures for Power and Energy Applications*, 2014: p. 15-45.

112. Karimi-Ghartemani, M., B.-T. Ooi, and A. Bakhshai, "Application of enhanced phase-locked loop system to the computation of synchrophasors.", *IEEE Transactions on Power Delivery,* 2011. **26**(1): p. 22-32.

113. Karimi-Ghartemani, M., "Linear and pseudolinear enhanced phased-locked loop (EPLL) structures.", *IEEE transactions on industrial electronics*, 2014. **61**(3): p. 1464-1474.

114. Ferreira, R., R.E. Araújo, and J.P. Lopes, "A comparative analysis and implementation of various PLL techniques applied to single-phase grids.", *Energetics (IYCE),* 3rd International Youth Conference on. 2011. IEEE.

115. Ghartemani, M.K., et al., "Problems of startup and phase jumps in PLL systems.", *IEEE Transactions on Power Electronics*, 2012. **27**(4): p. 1830-1838.

116. Kleeman, L. "Understanding and applying Kalman filtering.", *Proceedings of the Second Workshop on Perceptive Systems,* Curtin University of Technology, Perth Western Australia (25-26 January 1996). 1996.

117. Reza, M.S., M. Ciobotaru, and V.G. Agelidis, "Instantaneous power quality analysis using frequency adaptive Kalman filter technique.", *Power Electronics and Motion Control Conference (IPEMC), 2012 7th International*. 2012. IEEE.

118. Reza, M.S., M. Ciobotaru, and V.G. Agelidis, "Frequency adaptive instantaneous power quality analysis using frequency locked loop based Kalman filter technique.", *Power Electronics for Distributed Generation Systems (PEDG),* 2012 3rd IEEE International Symposium on. 2012. IEEE.